

Dear Anonymous Referee #2,

We would like to thank both reviewers for having taken your time to read our manuscript so thoroughly. We also highly appreciate your critics, comments and suggestions. We have addressed the points raised, and we believe that the manuscript has improved considerably owing to taking into account your comments.

Yours sincerely,

Quynh Nguyen on behalf of the authors

[Interactive comment on “Seasonal variation of atmospheric particle number concentrations, new particle formation and atmospheric oxidation capacity at the high Arctic site Villum Research Station, Station Nord” by Q. T. Nguyen et al.](#)

[Anonymous Referee #2](#)

[Received and published: 23 May 2016](#)

The manuscript presents an analysis of aerosol characteristics at the high-Arctic site Station Nord in Greenland, based on continuous measurements during 2010–2013 (concentrating on year 2012). The focus of the manuscript is in analysis of new particle formation (NPF) events. Ambient conditions favoring NPF at the site are reported based on case-studies, and NPF events are also analyzed with respect to source areas based on air mass back-trajectories. The dataset presented in the manuscript is interesting, highlighting the importance of atmospheric NPF to the aerosol number even in the remote Arctic regions. This work is within the scope of Atmospheric Chemistry and Physics, and could be considered for publication after the comments below have been taken into account.

My major concern is the analysis of the airmasses in relation to the three NPF events presented in the paper. The arrival times of the air mass back-trajectories shown in Figure 7 do not seem to coincide with the NPF events presented in Figure 6. The first air mass shown arrives in-between of the double event A and all the other airmasses of Fig. 7 on the midnight following the events A, B and C. I don't see how any conclusions on aerosol and trace gases measured at Station Nord during these three NPF events could be drawn based on the airmasses shown in Fig 7. Therefore, the analysis of the whole of Section 3.2.3 should be redone by analysing airmasses arriving to the station at the start of the NPF event or at some other relevant time during the event.

Authors' response: We thank you for pointing out our errors in calculating HYSPLIT. We have now re-calculated the backwards trajectories hourly during the entire events, and found that the onset or interruption of the events might be explained by changes of air masses, but not really altitude. We have thereby re-written the entire section on trajectories. Please see Section 3.2.3 for the revision.

Other general comments:

1) Page 2, lines 3–4: “only nucleation and Aitken-mode particles were observed during the summer months”. Based on Figures 3–4 and Table 1, this does not seem to be the case. There are clearly particles larger than 100 nm present during all the months, although the concentrations of accumulation mode particles are lower during the summer.

Authors’ response: Thank you for your comment. We have revised the sentence to emphasize that nucleation and Aitken-mode particles are the predominant modes, but indeed not the only modes.

2) Also Asmi et al. (2016) reported on NPF observations at the Arctic measurement station Tiksi in northern Siberia. This could be added to the discussion on NPF observations in the Arctic (third paragraph of the Introduction section).

Authors’ response: Thank you very much for making us aware of this new publication. We have added Asmi et al. (2016) and relevant discussions to the Introduction section.

3) Page 4, lines 32–33: Is the local pollution source taken into account in the dataanalysis (for example by excluding data when the local wind direction is from the sector towards the pollution source)?

Author’s response: The local pollution is mainly from activities in the military camp and the car servicing the station, and sometimes from the airplanes arriving and leaving the station. However there is currently no systematic way of tracking or knowing the exact source/direction of pollution source in combination of wind direction analysis.

So, local pollution is currently deemed as where sudden elevated concentrations of NO_x are observed, and thereafter removed from the dataset. This indicator might not cover all types of local emissions that may occur, but at least the major ones.

4) Page 7, line 19: “during the time period from July 2010 to February 2013”. I suppose this should be “during 2012”, as was stated at the end of Section 2.2.2. Also, Figures 3–5 refer to the year 2012.

Author’s response: Actually data from the other years were also used to support the analysis of event statistics. Data from the other years were also used in Figure 8, 9 and Table 3 (together with data from 2012). It should already say on the figure/table captions, but we have added this sentence on page 6 about our use of data from the other years to make it explicit:

“Data from the other years were used to support the analysis of event statistics. Details of the data period used are provided in the caption of the relevant tables or figures.”

5) Page 8, line 27: This sentence is little unclear, consider revising to e.g. “Since nucleation mode particles were almost absent in April and relatively minor in May, the high median or average N values observed during these months were attributed to ..”

Authors’ response: This was indeed a bad sentence. We have removed it completely.

6) Could the analysis of Section 3.2.2 on the role of O₃ and NO_x in NPF made more general by including data during all the NPF events, instead of just using 3 case studies?

Also, comparison of the O₃ and NO_x between NPF and non-NPF days could provide useful information. Such analysis should probably be done seasonally in order to exclude the strong difference in NPF occurrence between summer and winter.

Authors’ response: Thank you for your comment. This is also in line with comment 22 from Referee 1.

To your concern upon the relation between O₃ and NPF, we have extended our analysis for all events in 2012, and included more statistics between O₃ concentrations and integrated nucleation mode (10-30 nm) particle number concentrations in one additional paragraph in section 3.2.2. We paste the paragraph below.

“The three events seemed to visually display an anti-correlation between, the concentration level of O₃ and the growth trend of smaller particles seemed to display an anti-correlation with early particle growth up to about 30 nm during Event A and Event B or about 40-50 nm in case of Event C. A Pearson correlation coefficient between O₃ concentration and integrated particle number concentrations for the nuclei mode range (10-30 nm) was calculated for each event observed during 2012, where O₃ data was available, and NO_x data was also available to eliminate local pollution spikes. Out of a total of 35 NPF events observed during 2012, 16 events (46% of total events) displayed a weak to moderate anti-correlation (Pearson correlation coefficient below -0.5) between the integrated particle number concentrations for the nuclei mode range (10-30 nm) and O₃, with an average coefficient value of -0.71. Meanwhile 12 events (34% of total events) displayed a negative correlation coefficient from -0.05 to -0.41, with an average value of -0.25; and 7 events (20% of total events) showed a positive correlation in the range of 0.09 to 0.44, with an average value of 0.30. In these later cases (54 % of total events), it can be deemed that there is no relationship between O₃ and the nucleation mode particle number concentrations. No positive Pearson correlation coefficient stronger than 0.5 was observed.”

We only mentioned NO_x since it has an effect on O₃ concentration, and also serves as an indicator of pollution sparks. However it should not have any other direct impacts on NPF events, and therefore we did not include any further analysis on this. We hope this is acceptable.

7) Page 14, lines 29–31: What were the criteria used in the removal of the local pollution episodes? An exceedance of certain NO_x level? Why weren't the episodes during August 2nd (Fig. 6) removed from the dataset, if they were identified as local pollution as discussed on lines 19–24 of page 14?

Authors' response: We defined local pollution episodes in Section 2.2.1. We have tried to re-write this part a bit as follows to make it clearer: "Subsequently, daily particle number size distributions were plotted to inspect any sudden increase in the particle number concentration above the background. If such sudden increase in particle number concentration peaked (without any detectable particle growth) coincided with sudden elevation of NO_x concentration, they were interpreted as local pollution events and excluded from the data set."

The episodes on August 2nd were meant as "examples". We have now added an explicit sentence (in Section 3.2.2, NO_x part) to explain that they were not used for data analysis. "Such episodes with NO_x interference are also demonstrated here as example and were not included in any calculations of data".

8) Page 15, lines 26–27: Are you certain that the airmasses descend from above the boundary layer in these two cases? At least for Event C the airmass arriving at 50 m height stays constantly below 250 m, which seems quite low to be above the boundary layer.

Authors' response: We have redone the HYSPLIT analysis, so this point no longer holds. Please see section 3.2.3 for our new analysis.

9) Page 15, lines 28–30: I don't fully understand how can the vertical mixing of the airmasses be inferred from Fig. 7 for the case of mid-day of June 19. According to the map, the two airparcels do not follow the same horizontal path, so even though they are at the same altitude at the same time on mid-day of June 19, they are not at the same location horizontally and therefore not interacting with each other.

Authors' response: This was indeed our mistake. We have redone the HYSPLIT analysis, so again this point no longer holds. Please see section 3.2.3 for the revised section instead.

10) Page 17, lines 1–2: Is the map of Figure 8 constructed using all the trajectories arriving at Station Nord during the year 2012? Is the number of trajectories big enough for drawing conclusions on the source areas of airmasses favouring NPF?

Authors' response: Thank you for your comment. We have added this additional sentence to the caption of Figure 8: "This figure uses all available data (62 events) from the study period July 2010 – February 2013." This is definitely not an overwhelming number, but represents our current best available data at the station to date. We hope providing this extra information on the size of the number of events would help the readers to judge the reliability of the map.

11) Page 17, lines 30–31: Asmi et al. (2016) reported similar NPF day frequency, 30–40%, during summer in Tiksi, Russia.

Authors' response: Once again, we thank you for providing us with this interesting paper. We have added a few sentences to the discussion highlighting the similarities and differences in our observations and Asmi et al. (2016).

12) In the conclusions, the statement on the close relationship of ozone to the particle growth (lines 18–19) seems hard to justify on the basis of the presented material, which is currently 3 case studies of NPF. What were the exact growth rates of 10–25 nm particles during these events? Could this analysis be made more thorough by including all the NPF days and showing the relationship between O₃ concentration and particle growth rates (see also my comment 6)?

Authors' response: Thank you for your suggestion. To perform a statistical analysis on ozone vs growth rate during all the new particle formation events is a very good idea and deserves attention in a manuscript focusing entirely on new particle formation. However, it was not the intention to completely dominate the focus on the new particle formation events in this paper. So, such an analysis would take too much space in this paper and we feel that it might be out of the current scope.

Technical comments:

Page 1, line 23: “focus” should be “focuses”

Authors' response: Thank you for noting this. It has been corrected accordingly.

Page 6, line 16: section number “2.2.2” should be “2.2.3”

Authors' response: Definitely! It has been corrected.

Page 12, line 5: “Fig. 9” should be “Fig. 6”

Authors' response: We have corrected the figure number accordingly

Page 17, line 30–31: “.. relatively higher compared to ..” should be “relatively high compared to ..”

Authors' response: Thank you for your suggestion. We have revised the sentence accordingly.

References:

Asmi, E., Kondratyev, V., Brus, D., Laurila, T., Lihavainen, H., Backman, J., Vakkari, V., Aurela, M., Hatakka, J., Viisanen, Y., Uttal, T., Ivakhov, V., and Makshtas, A.: Aerosol size distribution seasonal characteristics measured in Tiksi, Russian Arctic. *Atmos.Chem. Phys.* 16, 1271–1287, 2016

Interactive comment on *Atmos. Chem. Phys. Discuss.*, doi:10.5194/acp-2016-205, 2016.

1 **Seasonal variation of atmospheric particle number**
2 **concentrations, new particle formation and atmospheric**
3 **oxidation capacity at the high Arctic site Villum Research**
4 **Station, Station Nord**

5

6 Q.T. Nguyen^{1,2,3}, M. Glasius^{2,4}, L.L. Sørensen^{1,6}, B. Jensen¹, H. Skov^{1,5,6}, W. Birmili⁷, A.
7 Wiedensohler⁷, A. Kristensson⁸, J.K. Nøjgaard¹ and A. Massling^{1,6}

8 ¹ Department of Environmental Science, Aarhus University, 4000 Roskilde, Denmark

9 ² Department of Chemistry, Aarhus University, 8000 Aarhus, Denmark

10 ³ Department of Engineering, Aarhus University, 8200 Aarhus, Denmark

11 ⁴ Interdisciplinary Nanoscience Center (iNANO), Aarhus University, 8000 Aarhus, Denmark

12 ⁵ Institute of Chemical Engineering and Biotechnology and Environmental Technology, University
13 of Southern Denmark, 5230 Odense, Denmark

14 ⁶ Arctic Research Centre, Aarhus University, 8000 Aarhus, Denmark

15 ⁷ Leibniz Institute for Tropospheric Research, 04318 Leipzig, Germany

16 ⁸ Department of Physics, Lund University, Sweden

17

18 Correspondence to: Q.T. Nguyen (quynh@eng.au.dk)

19

20 **Abstract**

21 This work presents an analysis of the physical properties of sub-micrometer aerosol particles
22 measured at the high Arctic site Villum Research Station, Station Nord (VRS), northeast Greenland
23 between July 2010 and February 2013. The study focuses on particle number concentrations,
24 particle number size distributions, the occurrence of new particle formation (NPF) events and their
25 seasonality in the high Arctic, where observations and characterization of such aerosol particle
26 properties and corresponding events are rare and understanding of related processes is lacking.

1 A clear accumulation mode was observed during the darker months from October until mid-May,
2 which became considerably more pronounced during the prominent Arctic haze months from March
3 to mid-May. In contrast, ~~only~~ nucleation and Aitken-mode particles were predominantly observed
4 during the summer months. Analysis of wind direction and wind speed indicated possible
5 contributions of marine sources from the easterly side of the station to the observed summertime
6 particle number concentrations, while southwesterly to westerly winds dominated during the darker
7 months. NPF events lasting from hours to days were mostly observed from June until August, with
8 fewer events observed during the months with less sunlight March, April, September, and October.
9 ~~The results tend to indicate It was observed~~ that ozone (O₃) ~~is likely to play an important role in the~~
10 ~~formation and growth of new particles at the site during summertime might be weakly anti-~~
11 ~~correlated with particle number concentrations of the nucleation mode range (10-30 nm) in almost~~
12 ~~half of the NPF events, while no positive correlation was observed.~~ Calculations of air-mass back
13 trajectories using the Hybrid Single Particle Lagrangian Integrated Trajectory (HYSPLIT) model
14 for the NPF event days suggested that the onset or interruption of events could possibly be
15 explained by changes in air mass origin~~originated from other places and transported together with~~
16 ~~O₃ in air parcels from different heights of the boundary layer down to the station at ground level.~~ A
17 map of event occurrence probability was computed, indicating that southerly air masses from over
18 the Greenland Sea were more likely linked to those events.

19 1. Introduction

20 Climate change driven by anthropogenic greenhouse gas emissions is a global challenge. In the
21 Arctic, the warming climate has already led to an earlier onset of spring-ice melt, later freeze-up
22 and decreasing sea-ice extent (Zwally et al., 2002; Markus et al., 2009; Stroeve et al., 2012). The
23 reduction of the Earth's albedo due to ice loss subsequently impacts the radiative balance of the
24 Earth through a positive feedback, leading to further warming. As a result, the Arctic has been
25 considered a manifestation of global warming with the rate of temperature increase in the region
26 being twice as high as the rest of the world (IPCC, 2013; ACIA, 2005), up to 8 - 9 °C along the east
27 coast of Greenland (Stendel et al., 2008). In addition to long-lived greenhouse gases, short-lived
28 climate forcings including tropospheric ozone, aerosols and black carbon also play a significant role
29 affecting the radiative balance in the Arctic (Quinn et al., 2008; Bond et al., 2013; IPCC, 2013).

30 Aerosol particles influence the radiative balance in the Arctic in many ways, through their ability to
31 absorb and scatter incoming solar radiation or by acting as cloud condensation nuclei to form cloud
32 and fog droplets. The presence of low level liquid clouds above bright ice- and snow-covered
33 surfaces in the Arctic could lead to increasing near-surface temperature as opposed to a cooling

Field Code Changed

Field Code Changed

Field Code Changed

Field Code Changed

Field Code Changed

Field Code Changed

Field Code Changed

Field Code Changed

Field Code Changed

1 effect observed in most other global regions (Shupe and Intrieri, 2004; Bennartz et al., 2013),
2 though the effect is probably small (AMAP, 2011). At the same time, deposition of black carbon on
3 Arctic snow- and ice-covered surfaces accelerates surface heating and ice melting in early spring
4 (Hansen and Nazarenko, 2004; Flanner et al., 2007; Flanner et al., 2009). It is thus crucial to
5 investigate the dynamics of atmospheric aerosol particles observed in the Arctic (involving the
6 formation, concentration, physico-chemical properties, temporal variability and transport) to
7 understand their direct and indirect effects on the radiation budget.

8 It is well known that during each winter extending into spring, Arctic aerosol particles containing
9 mineral dust, black carbon, heavy metals, elements, sulfur and nitrogen compounds are detected in
10 elevated concentrations. This has been attributed to the annually recurring Arctic haze phenomenon,
11 which is related to distant latitude anthropogenic pollution (Li and Barrie, 1993; Quinn et al., 2002;
12 Ström et al., 2003; Heidam et al., 2004; Heidam et al., 1999; Nguyen et al., 2013). The focus was
13 thus on long-range transported aerosols, which are expected to be aged due to the long transport
14 distance from mid-latitude source regions.

15 A number of studies have reported in-situ formation of new aerosol particles in the Arctic, which
16 mostly involved new particle formation in the Arctic boundary layer. The first observations of the
17 occurrence of an ultrafine particle mode (< 20 nm) in the Arctic marine boundary layer during
18 summer and autumn were reported by Wiedensohler et al. (1996) and Covert et al. (1996).

19 Observations of small aerosol particles during the summer period have also been reported at the
20 Zeppelin mountain site, Svalbard (11.9°E, 78.9°N, 478 m a.s.l.) within the Arctic boundary layer
21 (Ström et al., 2003; Tunved et al., 2013). The current understanding on mechanisms of new particle
22 formation in the marine boundary layer over the Arctic Ocean is unclear, due to the low
23 concentration of nucleating agents such as sulfuric acid in the marine boundary layer (Pirjola et al.,
24 2000; Karl et al., 2012), in addition to the limited number of observational data. Growth of ultrafine
25 particles has been observed at Summit, Greenland (38.4°W, 72.6°N, 3200 m a.s.l.) (Ziemba et al.,
26 2010). Quinn et al. (2002) also found an increase in particle number concentrations during the
27 summer months at Barrow, Alaska (156.6°W, 71.3°N, 8 m a.s.l.), which was attributed to the
28 formation of smaller particles. A correlation between summertime particle number concentrations
29 and the biogenic production of methane sulfonate (MSA⁻) was shown, indicating that the production
30 of summertime particles may be associated with biogenic sulfur (Quinn et al., 2002). Similar
31 finding has been recently reported by Leaitch et al. (2013) based on observations from Alert,
32 Nunavut. Heintzenberg et al. (2015) observed newly formed small aerosol particles during several
33 cruises to the summer central Arctic Ocean and suggested that they could originate from around the
34 Arctic region, more specifically related to air masses passing by open waters prior to the

Field Code Changed

Field Code Changed

Field Code Changed

Field Code Changed

Field Code Changed

Field Code Changed

Field Code Changed

Field Code Changed

Field Code Changed

Field Code Changed

Formatted: Danish

Field Code Changed

Formatted: Danish

Field Code Changed

Formatted: Danish

Formatted: Danish

Formatted: Danish

Formatted: Danish

Formatted: Danish

Formatted: Danish

Field Code Changed

Field Code Changed

Field Code Changed

Field Code Changed

Field Code Changed

Field Code Changed

Field Code Changed

1 observation point. Asmi et al. (2016) also recently suggested that NPF was more common in marine
2 air masses compared to continental air flows.

Field Code Changed

3 Meanwhile, source regions of aerosol particles in the Arctic could be very different (Hirdman et al.,
4 2010). Barrow is mostly influenced by North America and Arctic basin with some Russian and
5 Siberian sources (Quinn et al., 2002). Summit, which is located above the planetary boundary layer,
6 receives frequent long-range transported pollution from North America and extensively from
7 Eurasia during wintertime (Kahl et al., 1997; Hirdman et al., 2010). The mountainous site Zeppelin
8 (Tunved et al., 2013) and the ground level site VRS (16°40'W, 81°36'N, 30 m a.s.l.) (Heidam et al.,
9 2004; Nguyen et al., 2013) both receive long range transported pollution predominantly from
10 Eurasia during winter and spring. Zeppelin is often located south of the Polar Front receiving
11 transport from the Atlantic Ocean during summer (Tunved et al., 2013). Svalbard is also influenced
12 by the Gulf Stream (Phyushkov et al., 2013) and surrounded by open sea during summertime. VRS
13 is influenced by the ice stream from the Arctic Ocean along the east coast of Greenland (Stendel et
14 al., 2008; Kwok, 2009) and surrounded by multi-year sea ice, with limited first-year ice along the
15 coast. Such differences could have considerable impacts on NPF events and also aerosol particle
16 properties, which requires investigations at high spatial resolution in the Arctic.

Field Code Changed

Field Code Changed

Field Code Changed

Field Code Changed

Field Code Changed

Field Code Changed

Field Code Changed

Field Code Changed

Field Code Changed

Field Code Changed

Field Code Changed

17 VRS, Station Nord is a unique coastal station located close to sea level, representing the conditions
18 of the high Arctic throughout the year. Until date, there is only one observation and characterization
19 of NPF events at Alert, Nunavut (Leaitch et al., 2013). ~~while u~~Understanding of particle size
20 distribution, seasonality as well as related mechanisms and processes of NPF events are thus
21 lacking from ~~such a~~ high Arctic regionsite.

Field Code Changed

22 This study aims to characterize the formation, concentration, physical properties and seasonality of
23 atmospheric aerosols based on particle number size distributions at VRS. The occurrence of NPF
24 events was investigated in details. The events were classified and analyzed together with ozone (O₃)
25 and nitrogen oxides (NO_x = NO + NO₂). Wind direction and wind speed were analyzed to
26 investigate the impacts of source regions on the observed seasonality of particle number size
27 distribution. The source regions of new particle formation were mapped based on calculations of air
28 mass back trajectories using the HYSPLIT model during event days and non-event days. A
29 probability map for NPF event occurrence was computed.

30 2. Methods

31 2.1. Measurement site

1 Aerosol particles and trace gases were measured at the measurement site “Flyger’s Hut”, VRS,
2 Station Nord in northeast Greenland (81°36’N, 16°40’W, 30 m a.s.l.). The site is located on a small
3 peninsula (Princess Ingeborgs Peninsula) at approximately 2.5 km southeast of a small Danish
4 military base housing a crew of five soldiers (**Fig. 1**). Electricity at “Flyger’s Hut” is supplied from
5 a local JET A-1 fuel generator located inside the military base. The remote location of the station
6 implies a minor, though unavoidable, contribution of local anthropogenic pollution originating from
7 the military camp. The station is surrounded by multi-year sea ice, with limited bare ground
8 occasionally and limited first-year ice along the coast of Greenland during the summer months. At
9 VRS, Station Nord, polar sunrise is observed in the end of February, while polar day prevails from
10 mid-April to the beginning of September and polar night prevails from mid-October to the end of
11 February.

12 **2.2. Instrumentation**

13 **2.2.1. Mobility Particle Size Spectrometer**

14 Measurement of particle number size distributions at Station Nord was initiated in July 2010 using a
15 TROPOS-type Mobility Particle Size Spectrometer as described in Wiedensohler et al. (2012).
16 Briefly, the instrument consists of a medium Vienna-type Differential Mobility Analyzer (DMA)
17 followed by a butanol-based Condensation Particle Counter (CPC 3772 by TSI Inc., Shoreview,
18 USA). The DMA design is described in Winklmayr et al. (1991). The system is operated at 1 l min⁻¹
19 aerosol flow rate and 5 l min⁻¹ sheath air flow rate. The DMA sheath flow is circulated in closed
20 loop, facilitated by a regulated air blower. This technical setup allows measurements across a
21 particle size range from 10 to 900 nm in diameter. The time resolution of the instrument is 5 min,
22 including up-scan and down-scan.

23 The instrument was specifically designed to allow long-term operation with minimum maintenance
24 as follows. The DMA sheath air flow rate was continuously measured using a calibrated mass flow
25 sensor. The DMA aerosol flow rate was monitored by a pressure drop measurement over a
26 calibrated capillary. A computer-based control program adjusted the sheath air flow rate after each
27 measurement of the particle number size distribution. Systematic deviations in the sample flow rate,
28 which was controlled by a critical orifice in the CPC were monitored and corrected for in the
29 successive size distribution evaluation. Additionally, absolute pressure was measured at the inlet of
30 the system to detect any substantial technical problems such as clogging of the inlet. Temperature
31 and relative humidity (RH) were monitored at several positions inside the instrument. The RH

Field Code Changed

Field Code Changed

1 inside the DMA is the most critical parameter, since excessive moisture would allow particles to
2 grow much beyond their nominal dry diameter. At VRS, Station Nord, RH is usually not a critical
3 issue, as the climate is cold and arid with low humidity most of the year. The temperature in the
4 laboratory is mostly considerably higher than outdoor temperature, implying that substantial drying
5 of the aerosol is not needed most of the time during sample intake into the laboratory.

6 Sampling was provided from a conductive flow tube. An air blower was used to suck a main air
7 flow (much higher than the sample flow) into the main sampling inlet, and the air sampling was
8 probed from this main air flow using a ¼ inch tubing directed into the main air flow. The main
9 sampling inlet was not heated; however no icing issue was observed for the inlet. The main
10 sampling inlet did not have any size cut-off. Sampling was performed at standard conditions of
11 about 20 °C.

12 2.2.2. Data processing

13 The raw particle electrical mobility distributions collected by the mobility particle size spectrometer
14 were processed by a linear inversion algorithm presented in Pfeifer et al. (2014). Specific DMA
15 transfer function was used for inverting the data, while CPC efficiency and diffusion losses were
16 corrected for during the inversion.

17 As a first part of quality control, any data associated with DMA excess air RH above 50 % and
18 sheath air temperature above 30 °C were excluded from further data analysis, as recommended by
19 ACTRIS and WMO-GAW ([http://www.wmo-gaw-wcc-aerosol-physics.org/recommen-](http://www.wmo-gaw-wcc-aerosol-physics.org/recommendations.html)
20 [dations.html](http://www.wmo-gaw-wcc-aerosol-physics.org/recommendations.html)). These incidents were only observed on a few days during the study period.

21 Subsequently, daily particle number size distributions were plotted to inspect any sudden increase in
22 the particle number concentration above the background. If ~~short-lived such sudden increase in~~
23 ~~particle number concentration peaked~~ (without any detectable particle growth) coincided with
24 sudden elevation of similar peaks of NO_x concentration, they were interpreted as local pollution
25 events and excluded from the data set. These local pollution events were observed throughout the
26 year at the station. **Fig. 2** shows the extent of data coverage over the study period. Gaps in the data
27 set (most notably in 2011) were due to excluded data with flow uncertainties. 2012 was the year
28 with the best data coverage, with the lowest percentage of ca. 78 % in March while exceeding 90 %
29 in most other months. The year 2012 was therefore chosen to examine the seasonality of Arctic

Field Code Changed

Field Code Changed

1 aerosols in details. Data from the other years were used to support the analysis of event statistics.
2 Details of the data period used are provided in the caption of the relevant tables or figures.

3 **2.2.32. Gas phase and meteorological parameters**

4 O₃ was measured using an API photometric O₃ analyzer (M400). The results were averaged to a
5 time resolution of 30 min. The detection limit was 1 ppbv with an uncertainty of 3 % and 6 % for
6 measured concentrations above and below 10 ppbv, respectively. The uncertainties were calculated
7 at 95 % confidence interval.

8 NO_x was averaged to a time resolution of 30 min (Teledyne API M200AU, San Diego, CA) with a
9 precision of 5 % and a detection limit of 150 ppt. The calibration was checked weekly using 345
10 ppb NO span gas while zero gas was added each 25 hour. NO_x was sampled at a flow rate of 1 l
11 min⁻¹. Coverage of O₃ and NO_x data in this study are indicated as the corresponding blue and red
12 line in **Fig. 2**.

13 Wind speed and wind direction data were obtained from a sonic anemometer (METEK, USA-1,
14 heated) for the period from April 2011 to April 2013. The sonic is placed on a horizontal boom at
15 the top of a 9 meter mast. The mast is situated about 36 m east-southeast from the measurement hut
16 at ca. 62 meter asl. This means that the fetch limited wind direction is 300 degree where the hut (2.8
17 m) is an obstacle. The area is flat for 10-20 km in all wind directions. In winter periods fewer data
18 were obtained due to frost on the anemometer when temperature was below approximately -35 °C.

19 **2.3. Classification of new particle formation events**

20 NPF events were identified and classified following a scheme adapted from Dal Maso et al. (2005).
21 A brief description is given here.

22 A plot was compiled for each day with available particle number size distribution data, plotting the
23 particle diameter on the y-axis, time of the day (from midnight to midnight) on the x-axis, with the
24 particle number concentration in each size interval displayed as a contour plot. A panel of three
25 persons performed visual inspection, identification and classification of data to avoid subjective
26 bias. In order to be classified as an event day, the occurrence of a new particle mode below 20 nm
27 with concentrations substantially higher than during the previous hours must be observed. If a clear
28 diameter growth of newly formed particles could be traced for several hours, that specific day
29 would be classified as a class I event day. If the growth of newly formed particles was not
30 continuous over several hours, that specific day would be classified as a class II event day. The

Field Code Changed

1 identified NPF events at Station Nord typically lasted from hours to days. In case of a multi-day
2 event, only the first day, during which the event onset was identified, was counted as an event day.
3 The panel must agree on all classifications, otherwise the specific day would be classified as an
4 undefined event. Other options for classifications are non-event day or bad data in case of missing
5 data or observed instrumental problems.

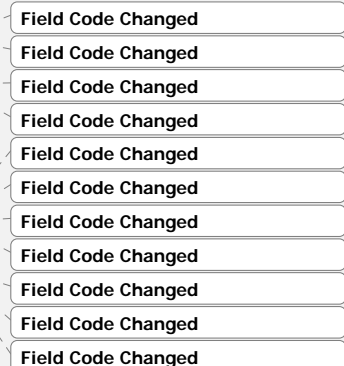
6 **3. Results and Discussion**

7 This section presents the observed overall seasonality of particle number size distributions
8 measured at VRS, Station Nord during the time period from July 2010 to February 2013, with an
9 analysis of NPF event cases together with the atmospheric oxidation capacity at the station.
10 Analysis of local wind speed, wind direction and air mass back trajectories was used to support the
11 interpretation of the seasonality of particle number size distributions and the dynamics of NPF
12 events.

13 **3.1. Particle number size distributions and seasonality**

14 **3.1.1. Overview**

15 A clear seasonality of particle number size distributions was observed during 2012 (**Fig. 3-4**). A
16 persistent accumulation mode appeared in the end of September, which became more prominent in
17 the end of February lasting until mid-May. The Arctic summer (June - August) was coupled with a
18 higher abundance of nucleation mode and Aitken mode aerosol particles and a very low abundance
19 of accumulation mode particles (Table 1). The small particles were also observed to a lesser extent
20 in September and only during one episode in mid-October. This observation of strong seasonality
21 was supported by observations from the available scattered data in the other years 2010, 2011 and
22 2013. The elevated concentrations of accumulation mode particles observed in this study generally
23 followed the varying pattern of aged total suspended particles during the Arctic haze period
24 previously reported at VRS, Station Nord (Heidam et al., 2004; Nguyen et al., 2013) and other
25 Arctic stations (Quinn et al., 2002; Ström et al., 2003). It should also be noted that the sun rises in
26 the end of February at Station Nord, so the period thereafter is affected by photochemical processes.
27 Observations of smaller particles during this period were in accordance with previous studies in the
28 Arctic (Ström et al., 2003; Tunved et al., 2013; Wiedensohler et al., 1996; Covert et al., 1996;
29 Quinn et al., 2002; Heintzenberg et al., 2015; Leaitch et al., 2013). During this period, the Arctic is
30 considerably cleaner with respect to long-range transport of atmospheric pollutants and
31 characterized by constant daylight.



3.1.2. Statistics of the particle number size distribution

Fig. 4 and **Table 1** describe detailed statistics of the particle number size distributions measured at the site, ~~especially regarding~~ showing the prominent accumulation mode during February - May and the prominent nucleation/Aitken mode during June - August. **Table 2** provides detailed median and average particle number concentration (N), particle volume concentration (V) and particle mass concentration (M) values calculated using the particle number size distributions at VRS, Station Nord during 2012. Higher values of median or average N were observed from April to September. During this period, largest discrepancies between the median and the average values were also found, especially during June (Median N = 137 particles cm⁻³, Average N = 277 particles cm⁻³) and August (Median N = 227 particles cm⁻³, Average N = 313 particles cm⁻³). This was attributed to the occurrence of intense NPF events during these months (**Fig. 3**), skewing the average N towards higher values compared to median N. June and August also showed highest average N in 2012, followed by May, April and July, whereas the months with the lowest average N were October, November and December. ~~Since nucleation mode particles were almost absent in April and relatively minor in May, their corresponding high median or average N values observed were attributed to the elevated presence of the pronounced accumulation mode during these two months (Fig. 3).~~

Newly formed particles are usually high in number and therewith significantly influence the total number concentration N as discussed above; however they do not contribute considerably to the total particle volume concentration V. As a result, June and August were among the months with the lowest median or average V together with other sunlit months July and September (**Table 2**). In contrast, the highest median and average V were observed during the most prominent haze months March - May. Simple log-normal fitting applied to the accumulation mode observed in the monthly particle number size distributions in 2012 revealed a geometrical mean diameter of approximately 170 nm during the winter and spring months (**Table 1**). This indicates that the particles can originate from distant locations due to their longer lifetimes determined by their size (Massling et al., 2015).

The total particle mass concentrations M were derived directly from the total particle volume concentration V, assuming a density of 1.4 g cm⁻³ and particle sphericity. Average monthly estimates of M ranged from 0.21 µg m⁻³ (June) to 1.58 µg m⁻³ (March) (**Table 2**).

Field Code Changed

1 Similar distribution of the major modes was also observed at the Zeppelin mountain site by Tunved
2 et al. (2013). However, the nucleation mode -- Aitken mode observed during the summer months
3 seemed considerably more pronounced at VRS, Station Nord compared to Zeppelin. This indicates
4 higher number concentrations of smaller particles at Station Nord, which were visible until October
5 (**Fig. 3-4**). In regards of the total particle mass concentration, Tunved et al. (2013) reported summer
6 M mostly below $0.2 \mu\text{g m}^{-3}$ and higher M below $0.8 \mu\text{g m}^{-3}$ observed at Zeppelin during the
7 prominent haze months March - April (with an assumed lower density of 1 g cm^{-3}). Clearly, the
8 particle mass concentration at Villum Research Station, VRS, Station Nord seemed comparable
9 during summer while showing higher concentrations during the Arctic haze months compared to
10 Zeppelin with different assumed particle densities already accounted for. This difference between
11 the two sites could be partially attributed to their different locations as discussed above. In addition,
12 the study periods and lengths of the studies were also different, as the Zeppelin data was averaged
13 for March 2000 - March 2010 whereas the descriptive distribution statistics in this work was
14 derived solely from data in 2012. Nevertheless, similar observations at both stations show the
15 consistent and predictable annual behavior of the particle number size distributions in the Arctic.

16 **3.1.3. Impacts of seasonal wind pattern**

17 Analysis of wind direction and wind speed was performed to investigate the impacts of wind pattern
18 on the particle number size distributions at the station. **Fig. 5** demonstrates monthly wind roses
19 during 2012, where two distinct patterns could be identified during the darker (September - April)
20 and the summer (June - August) period. The early haze months (January and February) and the
21 prominent haze months (March and April) showed prevailing wind arriving from the southwesterly
22 to westerly direction. During May, some northerly wind was observed while the frequency of
23 southwesterly wind seemed to decrease. During the summer period (June - August), when smaller
24 and freshly formed particles were observed, easterly wind became more prominent, especially
25 during July and August. September marked a prompt change in the wind direction back to
26 southwesterly direction. The wind speed became higher during November - December, which is
27 probably due to increasing katabatic winds from the ice sheet. During the other years 2011 and
28 2013 (data not shown), considerably similar patterns were observed for the corresponding months.

29 Earlier studies on source apportionment of total suspended particles (TSP) observed during the
30 Arctic haze period at VRS mostly identified Siberian industries and long-range transport from mid-
31 latitudes as major factors (Nguyen et al., 2013; Heidam et al., 2004) . However, the wind pattern

Field Code Changed

Field Code Changed

Field Code Changed

Field Code Changed

1 shown here may indicate an immediate impact of the adjacent southwesterly to westerly regions
2 contributing to the properties of particles prior to arrival at the station.

3 Based on the summer wind pattern, the smaller particles observed during June - August were
4 probably linked to sources from the easterly side of the station, with some marine contribution.

5 During summer, the marine contribution from the easterly direction is possibly driven by the retreat
6 of sea-ice cover, which exposes areas of open waters (“open leads”) and melt water on top of sea
7 ice to wind stress, especially along the coastal line of Greenland due to the presence of first-year-ice

8 in these regions. This would result in enhanced primary emissions of sea spray particles (Korhonen
9 et al., 2008). Surface active organic species in the ocean surface layer, which are more abundant due

10 to increased biological activity during summer, could also be released into the atmosphere by
11 bubble bursting (Middlebrook et al., 1998; Tervahattu et al., 2002) and become mixed with other

12 sea spray particles. It was suggested by Sellegri et al. (2006) that this could also alter the number
13 size distributions of particles. Another study by Karl et al. (2013) proposed that new nanoparticles

14 in the high Arctic could be marine granular nanogels injected into the atmosphere from evaporating
15 cloud droplets. Recent analysis of particle number size distributions and back trajectories during

16 summer cruises in the Arctic by Heintzenberg et al. (2015) also showed a ~~strong~~high coupling of
17 newly formed particles and the traveling of air masses over open water. At the same time, it must be

18 noted that wind measurements using the sonic anemometer were confined to local observations at
19 ground level, which according to radio sound measurements by Batchvarova et al. (2013), do not

20 capture activities such as transport of air masses at higher altitudes, or ~~regional transport of air~~
21 ~~masses-transport from a broader region~~. The extent of wind impacts on the particle size distributions

22 at the station is thus not well constrained.

23 Previous studies reported a dependence of particle number concentrations on wind speed in the
24 Arctic (Leck et al., 2002) and North Atlantic (Odowd and Smith, 1993). However, in this study the

25 accumulation mode particles (110 - 900 nm) only showed positive correlation with wind speed
26 during eight out of 12 months of 2012 with a moderate Pearson correlation coefficient range of 0.05

27 - 0.38. The reason could be partly attributed to the larger size ranges (500 nm up to 16 µm in
28 diameter) measured in the other studies, which are more influenced by wind speed.

29 **3.2. New particle formation events**

30 **3.2.1. Description of exemplary NPF events**

Field Code Changed

Field Code Changed

Field Code Changed

Field Code Changed

Field Code Changed

Field Code Changed

Field Code Changed

Field Code Changed

Field Code Changed

1 NPF events were observed at the station during the sunlit months, especially during the summer
2 months June – August, though events were also identified during the months with relatively low
3 sunlight March and October. The onset of NPF events was observed during various hours of the day
4 ~~(Supplementary Fig. 1) during the summer months, in combination with very small variations in~~
5 ~~solar flux during the day.~~ Examples of three events were shown in **Fig. 6**. As apparent from the
6 figure, the events showed clear but slow growth over considerably long periods up to a few days.

7 3.2.2. The role of atmospheric oxidants

8 **Fig. 6** also shows an overlay of O₃, NO and NO_x on the NPF event plots to allow analysis of the
9 role of atmospheric oxidants during those events.

10 Ozone

11 O₃ shows a strong seasonality in the Arctic troposphere with maximum springtime concentration
12 observed in the free troposphere, which is however poorly understood (Monks, 2000; Law and
13 Stohl, 2007). It has long been indicated that tropospheric O₃ in the Arctic is enriched from intruding
14 stratospheric air masses (Gregory et al., 1992; Gruzdev and Sitnov, 1993). A recent model study has
15 also suggested that summertime photochemical production of O₃ by NO_x in the Arctic could also be
16 a dominant source (Walker et al., 2012). This was attributed to NO_x emissions from the thermal
17 decomposition of the long-lived reservoir species peroxyacetyl nitrate (PAN) during summer (Fan
18 et al., 1994). Meanwhile, transport from mid-latitude source regions could also contribute to the O₃
19 budget in the Arctic during autumn and winter (Walker et al., 2012). Sources of O₃ in the Arctic
20 could therefore be a combination of different factors, including among others stratospheric
21 influence, local production and transport from mid-latitude sources. Finally, surface O₃ is also
22 depleted every spring due to reactions with Br atoms ~~released from sea-ice and surface snow~~ (Barrie
23 et al., 1988; Simpson et al., 2007; Skov et al., 2004; Bottenheim et al., 1990; Pratt et al., 2013;
24 Abbatt, 2013), similar to O₃ depletion in the stratosphere.

25 In this work, O₃ was used as a tracer of atmospheric chemical processes, and the concentration of
26 O₃ was found to be related to the formation and growth of new particles at Station Nord during
27 summer based on case studies of NPF events in 2012 (**Fig. 69**).

28 **Event A, Fig. 6:** Event A is in fact a “double” event, with the first event occurring over June 15 - 16
29 followed by another event starting on June 17 with traceable growth until June 20.

Field Code Changed

Field Code Changed

Field Code Changed

Field Code Changed

Field Code Changed

Field Code Changed

Field Code Changed

Field Code Changed

Field Code Changed

Field Code Changed

1 During June 15, the O₃ level (black line) increased considerably to ~45 ppbv, which was
2 significantly higher than the average summer (June - August, 2012) concentration of O₃ (~26 ppbv).
3 As the NPF event on June 15 started followed by particle growth up to ~25 nm, the O₃ level
4 dropped dramatically, then somewhat stabilized when the approximate mean particle size reaches
5 the lower Aitken mode. The next drop in O₃ concentration (from ~37 ppbv to ~27 ppbv) coincided
6 with the occurrence of the second NPF event observed around noon of June 17. As the new particles
7 grew beyond ~30 nm in diameter, the O₃ concentration seemed to stabilize again.

8 In the late hours of June 19, the O₃ concentration suddenly dropped by ~5 ppbv, coinciding with an
9 interruption of the event. By midday June 20, the O₃ concentration increased back to the pre-
10 interruption level, while that interrupted event also seemed to be brought back to the station. It was
11 unclear if this drop of O₃ concentration on June 19 was associated with any NPF, as nucleation
12 sized particles were also observed for a few hours during early hours on June 20. However, a full
13 justification of this observation was not possible due to the detection limit of the Mobility Particle
14 Size Spectrometer system (~10 nm) confining to only aged nucleation particles. Another
15 explanation could be that both O₃ and the nucleation event were transported to the station from a
16 common source, with the interruption probably indicating for instance a displacement of air mass.

17 ~~It has been observed that O₃ depletion occurs only when filterable bromide fBr is present, which is
18 in agreement with the evidence that O₃ is removed by Br atoms (Skov et al., 2004; Goodsite et al.,
19 2004; Goodsite et al., 2013). NPF at coastal location has also been found related to iodine oxides
20 (O'Dowd et al., 2002; McFiggans et al., 2010; Mahajan et al., 2011; Saiz-Lopez and von Glasow,
21 2012). This study was however unable to investigate the possible impact of halogen chemistry, due
22 to a lack of relevant measurement data.~~

23 During *Event A* case study, the NO and NO_x level remained mostly below 0.1 ppbv. This was
24 approximately the background level of NO_x at Station Nord throughout the year. NO and NO_x
25 concentration did not seem to relate to O₃ concentration level, or observations of new particle
26 formation events.

27 **Event B, Fig. 6:** This *Event B* on August 2 showed that a lower level of O₃ concentration (~25
28 ppbv) could also be associated with a new particle formation event. During the event, the episode of
29 traceable particle growth lasted for approximately 12h, coinciding with a concurrent drop of the O₃
30 concentration. This event was also considerably less intensive in regards of particle number

Field Code Changed
Field Code Changed
Field Code Changed
Field Code Changed
Field Code Changed
Field Code Changed
Field Code Changed

1 concentrations compared to *Event A*. Until the end of the event, particles were mostly below 30 nm
2 in size.

3 **Event C, Fig. 6:** During this event on August 9 - 10, new particle formation was also observed
4 together with lower O₃ concentrations (~25 ppbv), which was similar to *Event B*. The anti-
5 correlation between growth of newly formed particles and O₃ concentration was also observed
6 during this event. However, such anti-correlation was visible until particles almost reached 40-50
7 nm in diameter, which was higher than that observed during *Event A* and *Event B*. ~~The growth
8 seemed to be interrupted in the morning of August 10, allowing the concentration of the O₃ oxidant
9 to recover during that exact period back to values above 25 ppbv.~~

10 ~~As demonstrated with~~ The three events ~~seemed to visually display an anti-correlation between,~~ the
11 concentration level of O₃ ~~and the growth trend of smaller particles~~ seemed to display an anti-
12 correlation with early particle growth up to about 30 nm during *Event A* and *Event B* or about 40-50
13 nm in case of *Event C*. ~~A Pearson correlation coefficient between O₃ concentration and integrated
14 particle number concentrations for the nuclei mode range (10-30 nm) was calculated for each event
15 observed during 2012, where O₃ data was available, and NO_x data was also available to eliminate
16 local pollution spikes. Out of a total of 35 NPF events observed during 2012, 16 events (46% of
17 total events) displayed a weak to moderate anti-correlation (Pearson correlation coefficient below -
18 0.5) between the integrated particle number concentrations for the nuclei mode range (10-30 nm)
19 and O₃, with an average coefficient value of -0.71. Meanwhile 12 events (34% of total events)
20 displayed a negative correlation coefficient from -0.05 to -0.41, with an average value of -0.25; and
21 7 events (20% of total events) showed a positive correlation in the range of 0.09 to 0.44, with an
22 average value of 0.30. In these later cases (54 % of total events), it can be deemed that there is no
23 relationship between O₃ and the nucleation mode particle number concentrations. No positive
24 Pearson correlation coefficient stronger than 0.5 was observed.~~

25 It is generally agreed that particle nucleation involves sulfuric acid (H₂SO₄) via the oxidation of
26 SO₂ by the hydroxyl (OH) radical (Kulmala et al., 2001), while particle growth depends
27 considerably on vapor uptake and condensation of low-volatile organic vapor products produced by
28 photo-oxidation of volatile organic compounds (VOCs) (Donahue et al., 2011; Riipinen et al., 2011;
29 Riipinen et al., 2012). Naturally, O₃ is a major atmospheric oxidant, which also undergoes
30 photolysis to form the OH radical oxidant. These oxidants oxidize VOCs to form a variety of low-
31 volatile products. A reduction of O₃ could thus be an indirect indicator of increased availability and

Field Code Changed

Field Code Changed

Field Code Changed

Field Code Changed

1 thus uptake of low-volatile compounds, contributing to particle growth. Meanwhile, it should also
2 be noted that the role of halogen chemistry contributing to new particle formation is unknown, due
3 to a lack of relevant data as discussed above.

4 The source of VOCs at VRS, Station Nord is unclear. There might be some biogenic emissions of
5 VOCs at the station during summer, expected due to retreated snow and ice cover, exposed bare
6 ground and thus possibly increased biogenic activity. However, since this area is arid, this is
7 expected to be extremely limited. Meanwhile, the presence of VOC oxidation products such as
8 organic acids and organosulfates at the station has been reported by Hansen et al. (2014), though at
9 very low concentrations. The low mass or surface loading of organic materials (Nguyen et al., 2014)
10 and total suspended particles (Nguyen et al., 2013) and thus low condensation sink observed at the
11 station during summer would inhibit removal of small particles by condensation and also
12 coagulation to a lesser extent, thus allowing particle growth and prolonged NPF events. At the same
13 time, no considerable difference in particle mass or surface was observed at the onset of events
14 compared to the average particle mass or surface of the corresponding months during 2012.

~~15 As O₃ only seemed to inversely correlate with particle growth up to aged nucleation or lower~~
~~16 Aitken size, poor correlations were obtained between O₃ concentration and particle number~~
~~17 concentrations. Although the summer months in 2012 were event active, the Pearson correlation~~
~~18 coefficients between O₃ concentrations and particle number concentrations during June, July and~~
~~19 August were 0.37, 0.26 and -0.16, respectively. Meanwhile, it was found that O₃ correlated~~
~~20 positively with the observed particle volume concentrations during June (0.80), July (0.57), August~~
~~21 (0.38) and September (0.50), which probably indicated that oxidation by O₃ was no longer~~
~~22 important as particles reached larger size. At the same time, the possibility of the O₃ oxidant and/or~~
~~23 the new particle formation events being transported to the site in the same or different air masses~~
~~24 cannot be eliminated and will be examined further using HYSPLIT analysis.~~

25 NO_x

26 As mentioned above, sparks of particle formation, which did not grow further, were considered as
27 local pollution events, which related to NO_x emitted by the car engine during service of the station.
28 There was probably some additional contribution from emissions from the military base, which is
29 located at a distance of about 2.5 km from the measurement site. An example of such interference is
30 illustrated during the early hours of August 2 (*Event B*, **Fig. 6**), during which a higher NO_x
31 concentration of ~0.15 ppbv was detected together with a short episode of new particle formation

Field Code Changed

Field Code Changed

Field Code Changed

1 without further growth. Such interference could also be observed around midday of the same event
2 day (*Event B*, **Fig. 6**). In contrast, it must be noted that NO_x concentrations in the range ~0.1-0.2
3 ppbv were mostly not associated with any noticeable observations of new particle formation. Such
4 episodes with NO_x interference are also demonstrated here as example and were not included in any
5 calculations of data.

6 ~~During the late winter—spring months (March—May), episodes of depletion or complete removal of~~
7 ~~the surface layer O₃ and mercury in the Arctic occur due to reaction with atmospheric bromine~~
8 ~~released from sea ice and surface snow (Barrie et al., 1988; Bottenheim et al., 1990; Pratt et al.,~~
9 ~~2013; Abbatt, 2013; Abbatt et al., 2012; Skov et al., 2004). The concentration of O₃ then is so low~~
10 ~~that it can no longer oxidize NO and NO₂. Local NO_x emissions thus seemed to relate to the intense~~
11 ~~burst of small particles which lasted for hours. Removal of these episodes resulted in several~~
12 ~~noticeable gaps in the data set, especially in March and May 2012 (Fig. 3).~~

13 The summer period June - August was associated with a lower level of background NO_x (NO_x ~0.1
14 ppbv) compared to the rest of the year (NO_x ~0.2 ppbv). NO_x emissions into the Arctic atmosphere
15 other than the direct local anthropogenic emissions could originate from the thermal decomposition
16 of PAN, which is the major atmospheric NO_x reservoir species (Singh et al., 1995). This process is
17 nevertheless limited by low temperature during winter and spring and low PAN levels during
18 summer (Beine and Krognnes, 2000). NO_x also contributes via photochemistry to the local formation
19 of tropospheric O₃ and thus enhances O₃ levels during summer (Walker et al., 2012; Beine and
20 Krognnes, 2000) ~~at the expense of NO_x concentrations. However, a direct relation between O₃ and~~
21 ~~NO_x during summertime was not observed (Fig. 6).~~

22 3.2.3 Analysis of air mass back trajectories

23 As mentioned above, the Mobility Particle Size Spectrometer system employed at VRS, Station
24 Nord is limited to particles larger than 10 nm in size, capturing only aged nucleation particles. It is
25 thus uncertain whether the formation of the freshly nucleated particles actually occurred at the site,
26 or if they were transported from elsewhere or produced aloft.

27 Air mass back trajectories were analyzed in order to investigate possible source regions for the
28 observed events. The trajectories were calculated using HYSPLIT (Draxier and Hess, 1998). The
29 model runs were based on meteorological data obtained from the Global Data Assimilation System
30 (GDAS), which is maintained by the US National Centers for Environmental Prediction (NCEP).

Field Code Changed

Field Code Changed

Field Code Changed

Field Code Changed

Field Code Changed

1 In order to facilitate the interpretation of the events shown in Figure 6, hourly air mass back-
2 trajectories were calculated going 72h to 48h backwards for air masses arriving at the station at
3 50 m and 500 m above sea level on the event days, which were discussed earlier in Fig. 6. The
4 trajectories were are presented in Fig. 7, with the names of the events kept consistent with those in
5 Fig. 6. Only the first two days (June 15–16) and the last two days (June 19–20) of Event A was
6 shown in Fig. 7. Calculations of air mass back trajectories were performed for ~~these two~~ three day
7 periods, in order to minimize the uncertainties associated with calculating longer trajectories ~~many~~
8 ~~days backwards.~~

9 As can be seen in Fig. 7, Event A, westerly air masses were arriving at the station during the hours
10 before the onset of the event. At 21h on June 15, air masses started to originate from the
11 southwesterly direction instead, which also marks the observation of the first NPF event. In fact,
12 during both NPF events identified on June 15 and June 17, during Event A, air masses seemed to be
13 fast-moving, originating from longer distances in the southwesterly direction. During the late hours
14 of June 17 to early June 19, the station started to receive more air masses arriving from northerly
15 direction (for example 19 June, 06:00 local time), which may associate with the faded nucleation
16 mode particles observed during this exact time period. The “interrupted period” observed on June
17 19-20 also seemed to overlap with the time period where air masses were locally confined (for
18 example 19 June, 15:00 local time), and nucleation mode particles started to be observed again as
19 the air masses started to arrive from a westerly direction instead (20 June, 16:00 local time). It
20 should be noted that this interrupted period was off by about 2 hours compared to changes in
21 HYSPLIT air mass trajectories, which might be attributed to uncertainties in HYSPLIT output,
22 especially for calculating air mass movement over small distances in an area with few
23 meteorological measurement data.

24 The trajectories for Event B (Fig. 7) show that from 5-18h on August 2, air masses seemed to arrive
25 constantly along the coastal line from the northerly direction (which is shown by the example of
26 August 2, 06:00 local time), compared to the non-event period on that same day, where air masses
27 were arriving from inland instead (August 2, 03:00 and 18:00 local time). The air masses thus might
28 involve the Arctic sea-ice region (Supplementary Fig. 2) and related sources such as open leads or
29 melted water on top of sea ice due to wind stress as discussed above.

30 At the same time, the onset of an observed event cannot always be traced using HYSPLIT air mass
31 back trajectories. For example, Event C was observed at the site around 0h on August 9 (Fig. 7,

1 *Event C* despite no clear changes in HYSPLIT air mass back trajectories. This was a rather weak
2 event which seemed to stem from particle size below 10 nm, which was not able to be captured by
3 the Mobility Particle Size Spectrometer. This also highlights the uncertainty with using HYSPLIT
4 to trace the onset of the NPF event, as the onset time might be only for particles above 10 nm in
5 diameter, whereas the air masses transporting particles below 10 nm in size might have arrived at
6 the site prior to this so-called onset time. On the other hand, the interruption of this *Event C* was
7 easier to trace, as it seemed to coincide with the time where the air masses were confined to the
8 inland westerly region prior to arriving at the station (August 10, 04:00 local time).

9 ~~Descending of air parcels from above the boundary layer was commonly observed on many event~~
10 ~~days, such as during *Event A* (June 15–16, 2012) and *Event C* (August 2, 2012) (Fig. 7). Strong~~
11 ~~vertical mixing could relate to an interruption of an event. For example, an episode of vertical~~
12 ~~mixing between the lower (red) and upper air parcels (blue) occurred around mid-day of June 19,~~
13 ~~2012 and lasted until the early morning hours of the following day (~15 hours in total) (Fig. 7). This~~
14 ~~could probably relate to the interrupted phase of particle growth and O₃ concentration earlier~~
15 ~~observed (~18 hours in total) (*Event A*, Fig. 6). The event interruption was also observed a few~~
16 ~~hours later, which was probably due to the travelled distance of the air mass between the vertical~~
17 ~~displacing point above the boundary layer and that reaching the station at the ground level.~~
18 ~~Nevertheless, as *Event A* resumed after the interruption on June 20, 2012, the observed lower~~
19 ~~Aitken-mode band seemed to continue the growth before the interruption (Fig. 6). Such observation~~
20 ~~probably indicated that the air parcels providing the source to the new particle formation events~~
21 ~~(and possibility also O₃) could be displaced from and then brought back to the station.~~
22 ~~Subsequently, this could indicate that the entire event was “transported” from aloft down to the~~
23 ~~ground level. Similarly, during *Event B* (August 2, 2012), vertical mixing between the upper air~~
24 ~~parcels (blue) and lower air parcels (red) occurred around noon time and lasted for ~12 hours (Fig.~~
25 ~~7). This seemed to relate to the NPF event occurring around the same time with roughly the same~~
26 ~~length (~12 hours) (*Event B*, Fig. 6).~~

27 ~~In fact, it was previously indicated that new particles could be formed aloft and subsequently~~
28 ~~transported to the ground level due to vertical mixing, leading to new particle formation events~~
29 ~~observed around noon time (Mäkelä et al., 2000; Crippa et al., 2012; Pryor et al., 2010). In another~~
30 ~~study by Wiedensohler et al. (1996), it was also suggested that the observed occurrence of particles~~
31 ~~smaller than 20 nm in diameter in the marine boundary layer over the Arctic pack ice could~~
32 ~~originate from higher altitudes. Assuming that the new particle formation events were transferred~~

Field Code Changed
Field Code Changed
Field Code Changed
Field Code Changed

1 ~~from aloft, it is possible that the vertical mixing with the upper air parcels could either interrupt an~~
2 ~~event or lead to observation of a new event at the site. This would depend on whether the displaced~~
3 ~~air parcels or the displacing air parcels are event active, or having the favorable conditions for the~~
4 ~~formation and growth of new particles, such as the presence of precursor gases. In contrast, an~~
5 ~~observed interruption during a new particle formation event such as during the early hours of~~
6 ~~August 10, 2012 (Event C, Fig. 6) was not always related to displacing air parcels. The interruption~~
7 ~~could instead relate to a change in the horizontal direction of the air parcels arriving at the station~~
8 ~~occurring around midnight of August 9, 2012 (Fig. 7).~~

9 Air mass back trajectories were also calculated three-days backwards, at one hour after the starting
10 time of each identified event using HYSPLIT, whereas for the other days, trajectories arriving at
11 12:00 p.m. local time were used. The region around Station Nord was split into one degree
12 latitudinal and six degree longitudinal grid boxes. Every time a trajectory passed one grid box, a
13 count was registered for that grid box. The probability of registering an event, when the air mass
14 originated from a specific grid box was obtained by dividing the total counts during event days by
15 the sum of total counts during event days, undefined and non-event days. The probability results are
16 shown in **Fig. 8**.

17 As apparent from the figure, the probability of observing an event at the station is low when the air
18 masses arrive from the southwesterly direction over Greenland. Other directions of air mass origin
19 however showed relatively similar probability of registering an event. A slightly higher probability
20 range was observed for southeasterly air masses that passed over region, where open waters and
21 melting ponds on ice are more likely to occur. As particles typically grow very slowly at Villum
22 Research Station, the time gap from particle nucleation occurring around 1.5 nm in diameter until
23 the point when they are observed at the site (~10 nm in diameter) could range from hours to days.
24 The corresponding probability for observing nucleation mode particles (~10 nm in diameter) at the
25 site should therefore serve as an indication of probable air mass origin of the grown nucleation
26 mode instead of freshly nucleated particles.

27 **3.2.4. Analysis of wind pattern during NPF events**

28 The wind pattern was also investigated on specific event days in 2011 and 2012 (figure not shown).
29 However, they were found very similar to the general wind patterns of the corresponding month or
30 period. Therefore, it is unlikely that any change in local wind direction during the specific event
31 days could have an impact on the occurrence of new particle formation events observed at the site.

1 This indicates the possibility of other factors, which may have changed during the event days
2 affecting new particle formation such as precursors. In fact, Quinn et al. (2002) indicated that the
3 abundant dimethyl sulfide (DMS) could affect particle production during summer, as evidenced by
4 a strong correlation between particle number concentrations and methanesulfonate (MSA)
5 concentrations (resulting from the oxidation of DMS). Similar observations were reported by
6 Leaitch et al. (2013). Other examples of factors influencing NPF are atmospheric oxidation capacity
7 and transport of air masses.

Field Code Changed

Field Code Changed

8 3.2.5. Event statistics

9 In general, the event days accounted for ~~175~~ - 38 % of the classified days during June - September,
10 with the highest percentages of event days observed in August (38 %) and July (33 %) (Table 3).
11 The period from June to early September was also the period during which longer events up to
12 several days were observed and most class I events were identified (Table 3).

13 The observed frequencies of event days during these months at VRS, Station Nord were relatively
14 higher compared to reported values from sub-Arctic stations during the same months, such as
15 Värriö (20 - 25%) (Kyro et al., 2014), Pallas (10 - 20 %) (Asmi et al., 2011) or Abisko (< 20 %)
16 (Vaananen et al., 2013), while overlap with the values 30-40 % reported by Asmi et al. (2016) from
17 Tiksi, Russian Arctic. In fact, the observed new particle formation events at these sub-Arctic
18 stations and other Nordic stations seemed to show a spring maximum of event occurrence
19 (Vehkamaki et al., 2004; Dal Maso et al., 2007; Kristensson et al., 2008), as opposed to the summer
20 maximum of events observed at VRS, Station Nord. Interestingly, Asmi et al. (2016) found the
21 highest NPF event frequencies in March (50%), whereas such frequency was only 10 % at VRS,
22 Station Nord during the same month. It should also be noted that Asmi et al. (2016) reported
23 measuring particle diameter from 7 nm at Tiksi, whereas only those above 10 nm were reported in
24 this study. ~~At the same time,~~ NPF events were still observed at the sub-Arctic stations Värriö ,
25 Pallas and Abisko during the darker months (November - February), though the fraction of event
26 occurrence was typically much lower compared to other seasons (Kyro et al., 2014; Asmi et al.,
27 2011; Vaananen et al., 2013). Notably, not a single event was observed at VRS, Station Nord during
28 the Arctic night in the absence of sunlight.

Field Code Changed

Field Code Changed

Field Code Changed

Field Code Changed

Field Code Changed

Field Code Changed

Field Code Changed

Field Code Changed

Field Code Changed

Field Code Changed

29 4. Conclusion

30 In this work, the seasonality of particle number size distributions, total particle number, volume and
31 mass concentrations was examined. A strong seasonal pattern was found, showing the abundance of

1 smaller particles during the sunlit period of the year, especially during summer and a persistent
2 accumulation mode during the darker months caused by long-range transport of particles to the
3 Arctic. Analysis of wind data showed a dominance of easterly winds during the summer months and
4 southwesterly winds during the darker months of the year.

5 ~~The observed NPF events at the station were investigated based on case studies, showing clear~~
6 ~~events lasting~~ from hours to days ~~with various onset time~~. O₃ was ~~possibly found closely~~ related
7 to the observed NPF events ~~observed at the station, especially in regards of particle growth with~~
8 ~~46% of NPF cases showing a weak to moderate anti-correlation (with an average coefficient value~~
9 ~~of -0.71) between O₃ concentration and integrated particle number concentrations for the nucleation~~
10 ~~mode range (10-30 nm), while no positive correlation was found and the remainder of events~~
11 ~~showed no correlation~~. Calculations of air mass back trajectories on the days with new particle
12 formation events using HYSPLIT indicated ~~that the onset or interruption of events might be~~
13 ~~explained by changes in air mass origin an aloft origin of air parcels arriving at the station on many~~
14 ~~event days. The overlaps between the occurrence of vertical displacing air masses and interruption~~
15 ~~of events observed at the measurement site further suggested that the event could be transported to~~
16 ~~or displaced from the site together with the air masses~~. Air masses arriving from the southwesterly
17 direction over Greenland were least linked to NPF event, whereas air masses arriving from
18 southeasterly direction over Greenland sea was associated with slightly higher probabilities.
19 Meanwhile, the local wind direction did not seem to relate to NPF events observed at the station

20 **Acknowledgements**

21 This work was financially supported by the Danish Environmental Protection Agency with means
22 from the MIKA/DANCEA funds for Environmental Support to the Arctic Region, which is part of
23 the Danish contribution to “Arctic Monitoring and Assessment Program” (AMAP) and to the
24 Danish research project “Short lived Climate Forcers” (SLCF). The findings and conclusions
25 presented here do not necessarily reflect the views of the Agency. This work was also supported by
26 the Nordic Centre of Excellence Cryosphere-Atmosphere Interactions in a Changing Arctic Climate
27 (CRAICC). The Villum Foundation is acknowledged for funding the construction of Villum
28 Research Station, Station Nord. The authors are also grateful to the staff at Station Nord for their
29 excellent support.

1 **References**

- 2 National Snow and Ice Data Center: <http://nsidc.org/>, access: 19 February 2016.
- 3 Abbatt, J.: Arctic snowpack bromine release, *Nat Geosci*, 6, 331-332, 2013.
- 4 Abbatt, J. P. D., Thomas, J. L., Abrahamsson, K., Boxe, C., Granfors, A., Jones, A. E., King, M. D.,
5 Saiz-Lopez, A., Shepson, P. B., Sodeau, J., Toohey, D. W., Toubin, C., von Glasow, R., Wren, S.
6 N., and Yang, X.: Halogen activation via interactions with environmental ice and snow in the polar
7 lower troposphere and other regions, *Atmos Chem Phys*, 12, 6237-6271, DOI 10.5194/acp-12-
8 6237-2012, 2012.
- 9 ACIA: (Arctic Climate Impact Assessment) Overview Report, Cambridge University Press,
10 Cambridge, 1042 p., 2005.
- 11 AMAP: Arctic Monitoring and Assessment Programme (AMAP), The Impact of Black Carbon on
12 Arctic Climate Oslo, 72, 2011.
- 13 Asmi, E., Kivekas, N., Kerminen, V. M., Komppula, M., Hyvarinen, A. P., Hatakka, J., Viisanen,
14 Y., and Lihavainen, H.: Secondary new particle formation in Northern Finland Pallas site between
15 the years 2000 and 2010, *Atmos Chem Phys*, 11, 12959-12972, DOI 10.5194/acp-11-12959-2011,
16 2011.
- 17 Asmi, E., Kondratyev, V., Brus, D., Laurila, T., Lihavainen, H., Backman, J., Vakkari, V., Aurela,
18 M., Hatakka, J., Viisanen, Y., Uttal, T., Ivakhov, V., and Makshtas, A.: Aerosol size distribution
19 seasonal characteristics measured in Tiksi, Russian Arctic, *Atmos Chem Phys*, 16, 1271-1287,
20 10.5194/acp-16-1271-2016, 2016.
- 21 Barrie, L. A., Bottenheim, J. W., Schnell, R. C., Crutzen, P. J., and Rasmussen, R. A.: Ozone
22 Destruction and Photochemical-Reactions at Polar Sunrise in the Lower Arctic Atmosphere, *Nature*,
23 334, 138-141, Doi 10.1038/334138a0, 1988.
- 24 Batchvarova, E. A., Gryning, S. E., Skov, H., Sørensen, L. L., Kirova, H., and Muenkel, C.:
25 Boundary-layer and air quality study at “Station Nord” in Greenland, 33rd International Technical
26 meeting on air pollution Modelling and its applications, August 26 – 30, Miami, Florida, USA,
27 2013,
- 28 Beine, H. J., and Krognes, T.: The seasonal cycle of peroxyacetyl nitrate (PAN) in the European
29 Arctic, *Atmos Environ*, 34, 933-940, Doi 10.1016/S1352-2310(99)00288-5, 2000.
- 30 Bennartz, R., Shupe, M. D., Turner, D. D., Walden, V. P., Steffen, K., Cox, C. J., Kulie, M. S.,
31 Miller, N. B., and Pettersen, C.: July 2012 Greenland melt extent enhanced by low-level liquid
32 clouds, *Nature*, 496, 83-86, 2013.
- 33 Bond, T. C., Doherty, S. J., Fahey, D. W., Forster, P. M., Berntsen, T., DeAngelo, B. J., Flanner, M.
34 G., Ghan, S., Kärcher, B., Koch, D., Kinne, S., Kondo, Y., Quinn, P. K., Sarofim, M. C., Schultz,
35 M. G., Schulz, M., Venkataraman, C., Zhang, H., Zhang, S., Bellouin, N., Guttikunda, S. K.,
36 Hopke, P. K., Jacobson, M. Z., Kaiser, J. W., Klimont, Z., Lohmann, U., Schwarz, J. P., Shindell,
37 D., Storelvmo, T., Warren, S. G., and Zender, C. S.: Bounding the role of black carbon in the

1 climate system: A scientific assessment, *Journal of Geophysical Research: Atmospheres*, 118, 5380-
2 5552, 10.1002/jgrd.50171, 2013.

3 Bottenheim, J. W., Barrie, L. A., Atlas, E., Heidt, L. E., Niki, H., Rasmussen, R. A., and Shepson,
4 P. B.: Depletion of Lower Tropospheric Ozone during Arctic Spring - the Polar Sunrise Experiment
5 1988, *J Geophys Res-Atmos*, 95, 18555-18568, Doi 10.1029/Jd095id11p18555, 1990.

6 Covert, D. S., Wiedensohler, A., Aalto, P., Heintzenberg, J., McMurry, P. H., and Leck, C.: Aerosol
7 number size distributions from 3 to 500 nm diameter in the arctic marine boundary layer during
8 summer and autumn, *Tellus B*, 48, 197-212, 1996.

9 Crippa, P., Petaja, T., Korhonen, H., El Afandi, G. S., and Pryor, S. C.: Evidence of an elevated
10 source of nucleation based on model simulations and data from the NIFTy experiment, *Atmos
11 Chem Phys*, 12, 8021-8036, DOI 10.5194/acp-12-8021-2012, 2012.

12 Dal Maso, M., Kulmala, M., Riipinen, I., Wagner, R., Hussein, T., Aalto, P. P., and Lehtinen, K. E.
13 J.: Formation and growth of fresh atmospheric aerosols: eight years of aerosol size distribution data
14 from SMEAR II, Hyytiälä, Finland, *Boreal Environment Research*, 10, 323-336, 2005.

15 Dal Maso, M., Sogacheva, L., Aalto, P. P., Riipinen, I., Komppula, M., Tunved, P., Korhonen, L.,
16 Suur-Uski, V., Hirsikko, A., Kurten, T., Kerminen, V. M., Lihavainen, H., Viisanen, Y., Hansson,
17 H. C., and Kulmala, M.: Aerosol size distribution measurements at four Nordic field stations:
18 identification, analysis and trajectory analysis of new particle formation bursts, *Tellus B*, 59, 350-
19 361, DOI 10.1111/j.1600-0889.2007.00267.x, 2007.

20 Donahue, N. M., Trump, E. R., Pierce, J. R., and Riipinen, I.: Theoretical constraints on pure vapor-
21 pressure driven condensation of organics to ultrafine particles, *Geophysical Research Letters*, 38,
22 Artn L16801 Doi 10.1029/2011gl048115, 2011.

23 Draxier, R. R., and Hess, G. D.: An overview of the HYSPLIT_4 modelling system for trajectories,
24 dispersion and deposition, *Aust Meteorol Mag*, 47, 295-308, 1998.

25 Fan, S. M., Jacob, D. J., Mauzerall, D. L., Bradshaw, J. D., Sandholm, S. T., Blake, D. R., Singh, H.
26 B., Talbot, R. W., Gregory, G. L., and Sachse, G. W.: Origin of Tropospheric Nox over Sub-Arctic
27 Eastern Canada in Summer, *J Geophys Res-Atmos*, 99, 16867-16877, Doi 10.1029/94jd01122,
28 1994.

29 Flanner, M. G., Zender, C. S., Randerson, J. T., and Rasch, P. J.: Present-day climate forcing and
30 response from black carbon in snow, *J Geophys Res-Atmos*, 112, Artn D11202, Doi
31 10.1029/2006jd008003, 2007.

32 Flanner, M. G., Zender, C. S., Hess, P. G., Mahowald, N. M., Painter, T. H., Ramanathan, V., and
33 Rasch, P. J.: Springtime warming and reduced snow cover from carbonaceous particles, *Atmos
34 Chem Phys*, 9, 2481-2497, 2009.

35 Goodsite, M. E., Plane, J. M. C., and Skov, H.: A theoretical study of the oxidation of Hg-0 to
36 HgBr₂ in the troposphere, *Environ Sci Technol*, 38, 1772-1776, 10.1021/es034680s, 2004.

37 Goodsite, M. E., Outridge, P. M., Christensen, J. H., Dastoor, A., Muir, D., Travnikov, O., and
38 Wilson, S.: How well do environmental archives of atmospheric mercury deposition in the Arctic

1 reproduce rates and trends depicted by atmospheric models and measurements?, *Sci Total Environ*,
2 452, 196-207, 10.1016/j.scitotenv.2013.02.052, 2013.

3 Gregory, G. L., Anderson, B. E., Warren, L. S., Browell, E. V., Bagwell, D. R., and Hudgins, C. H.:
4 Tropospheric ozone and aerosol observations: The Alaskan Arctic, *Journal of Geophysical*
5 *Research: Atmospheres*, 97, 16451-16471, 10.1029/91jd01310, 1992.

6 Gruzdev, A. N., and Sitnov, S. A.: Tropospheric Ozone Annual Variation and Possible
7 Troposphere-Stratosphere Coupling in the Arctic and Antarctic as Derived from Ozone Soundings
8 at Resolute and Amundsen-Scott Stations, *Tellus B*, 45, 89-98, DOI 10.1034/j.1600-0889.1993.t01-
9 1-00001.x, 1993.

10 Hansen, A. M. K., Kristensen, K., Nguyen, Q. T., Zare, A., Cozzi, F., Nøjgaard, J. K., Skov, H.,
11 Brandt, J., Christensen, J. H., Ström, J., Tunved, P., Krejci, R., and Glasius, M.: Organosulfates and
12 organic acids in Arctic aerosols: speciation, annual variation and concentration levels, *Atmos.*
13 *Chem. Phys. Discuss.*, 14, 4745-4785, 10.5194/acpd-14-4745-2014, 2014.

14 Hansen, J., and Nazarenko, L.: Soot climate forcing via snow and ice albedos, *P Natl Acad Sci*
15 *USA*, 101, 423-428, 10.1073/pnas.2237157100, 2004.

16 Heidam, N. Z., Wahlin, P., and Christensen, J. H.: Tropospheric gases and aerosols in northeast
17 Greenland, *J Atmos Sci*, 56, 261-278, [http://dx.doi.org/10.1175/1520-](http://dx.doi.org/10.1175/1520-0469(1999)056<0261:TGAAN>2.0.CO;2)
18 [0469\(1999\)056<0261:TGAAN>2.0.CO;2](http://dx.doi.org/10.1175/1520-0469(1999)056<0261:TGAAN>2.0.CO;2), 1999.

19 Heidam, N. Z., Christensen, J., Wahlin, P., and Skov, H.: Arctic atmospheric contaminants in NE
20 Greenland: levels, variations, origins, transport, transformations and trends 1990-2001, *Sci Total*
21 *Environ*, 331, 5-28, 10.1016/j.scitotenv.2004.03.033, 2004.

22 Heintzenberg, J., Leck, C., and Tunved, P.: Potential source regions and processes of aerosol in the
23 summer Arctic, *Atmos. Chem. Phys.*, 15, 6487-6502, 10.5194/acp-15-6487-2015, 2015.

24 Hirdman, D., Sodemann, H., Eckhardt, S., Burkhardt, J. F., Jefferson, A., Mefford, T., Quinn, P. K.,
25 Sharma, S., Strom, J., and Stohl, A.: Source identification of short-lived air pollutants in the Arctic
26 using statistical analysis of measurement data and particle dispersion model output, *Atmos Chem*
27 *Phys*, 10, 669-693, 2010.

28 IPCC: Climate Change 2013: The Physical Science Basis. Contribution of Working Group I to the
29 Fifth Assessment Report of the Intergovernmental Panel on Climate Change, Cambridge University
30 Press, Cambridge, United Kingdom and New York, NY, USA, 1535 pp., 2013.

31 Kahl, J. D. W., Martinez, D. A., Kuhns, H., Davidson, C. I., Jaffrezo, J. L., and Harris, J. M.: Air
32 mass trajectories to Summit, Greenland: A 44-year climatology and some episodic events, *J*
33 *Geophys Res-Oceans*, 102, 26861-26875, Doi 10.1029/97jc00296, 1997.

34 Karl, M., Leck, C., Gross, A., and Pirjola, L.: A study of new particle formation in the marine
35 boundary layer over the central Arctic Ocean using a flexible multicomponent aerosol dynamic
36 model, *Tellus B*, 64, Artn 17158 Doi 10.3402/Tellusb.V64i0.17158, 2012.

- 1 Karl, M., Leck, C., Coz, E., and Heintzenberg, J.: Marine nanogels as a source of atmospheric
2 nanoparticles in the high Arctic, *Geophysical Research Letters*, 40, 3738-3743, Doi
3 10.1002/Grl.50661, 2013.
- 4 Korhonen, H., Carslaw, K. S., Spracklen, D. V., Ridley, D. A., and Strom, J.: A global model study
5 of processes controlling aerosol size distributions in the Arctic spring and summer, *J Geophys Res-*
6 *Atmos*, 113, Artn D08211 Doi 10.1029/2007jd009114, 2008.
- 7 Kristensson, A., Dal Maso, M., Swietlicki, E., Hussein, T., Zhou, J., Kerminen, V. M., and
8 Kulmala, M.: Characterization of new particle formation events at a background site in Southern
9 Sweden: relation to air mass history, *Tellus B*, 60, 330-344, DOI 10.1111/j.1600-
10 0889.2008.00345.x, 2008.
- 11 Kulmala, M., Dal Maso, M., Makela, J. M., Pirjola, L., Vakeva, M., Aalto, P., Miikkulainen, P.,
12 Hameri, K., and O'Dowd, C. D.: On the formation, growth and composition of nucleation mode
13 particles, *Tellus B*, 53, 479-490, DOI 10.1034/j.1600-0889.2001.530411.x, 2001.
- 14 Kwok, R.: Outflow of Arctic Ocean Sea Ice into the Greenland and Barents Seas: 1979-2007, *J*
15 *Climate*, 22, 2438-2457, 10.1175/2008JCLI2819.1, 2009.
- 16 Kyro, E. M., Vaananen, R., Kerminen, V. M., Virkkula, A., Petaja, T., Asmi, A., Dal Maso, M.,
17 Nieminen, T., Juhola, S., Shcherbinin, A., Riipinen, I., Lehtipalo, K., Keronen, P., Aalto, P. P.,
18 Hari, P., and Kulmala, M.: Trends in new particle formation in eastern Lapland, Finland: effect of
19 decreasing sulfur emissions from Kola Peninsula, *Atmos Chem Phys*, 14, 4383-4396, DOI
20 10.5194/acp-14-4383-2014, 2014.
- 21 Law, K. S., and Stohl, A.: Arctic air pollution: Origins and impacts, *Science*, 315, 1537-1540, DOI
22 10.1126/science.1137695, 2007.
- 23 Leaitch, W. R., Sharma, S., Huang, L., Toom-Sauntry, D., Chivulescu, A., Macdonald, A. M.,
24 Salzen, K. v., Pierce, J. R., Bertram, A. K., Schroder, J. C., Shantz, N. C., Chang, R. Y. W., and
25 Norman, A. L.: Dimethyl sulfide control of the clean summertime Arctic aerosol and cloud, *Elem.*
26 *Sci. Anth.* , 1, 10.12952/journal.elementa.000017, 2013.
- 27 Leck, C., Norman, M., Bigg, E. K., and Hillamo, R.: Chemical composition and sources of the high
28 Arctic aerosol relevant for cloud formation, *J Geophys Res-Atmos*, 107, Artn 4135 Doi
29 10.1029/2001jc001463, 2002.
- 30 Li, S. M., and Barrie, L. A.: Biogenic Sulfur Aerosol in the Arctic Troposphere .1. Contributions to
31 Total Sulfate, *J Geophys Res-Atmos*, 98, 20613-20622, 10.1029/93JD02234, 1993.
- 32 Mahajan, A. S., Sorribas, M., Martin, J. C. G., MacDonald, S. M., Gil, M., Plane, J. M. C., and
33 Saiz-Lopez, A.: Concurrent observations of atomic iodine, molecular iodine and ultrafine particles
34 in a coastal environment, *Atmos Chem Phys*, 11, 2545-2555, 10.5194/acp-11-2545-2011, 2011.
- 35 Markus, T., Stroeve, J. C., and Miller, J.: Recent changes in Arctic sea ice melt onset, freezeup, and
36 melt season length, *J Geophys Res-Oceans*, 114, Artn C12024 Doi 10.1029/2009jc005436, 2009.
- 37 Massling, A., Nielsen, I. E., Kristensen, D., Christensen, J. H., Sørensen, L. L., Jensen, B., Nguyen,
38 Q. T., Nøjgaard, J. K., Glasius, M., and Skov, H.: Atmospheric black carbon and sulfate

1 concentrations in Northeast Greenland, *Atmos. Chem. Phys.*, 15, 9681-9692, 10.5194/acp-15-9681-
2 2015, 2015.

3 McFiggans, G., Bale, C. S. E., Ball, S. M., Beames, J. M., Bloss, W. J., Carpenter, L. J., Dorsey, J.,
4 Dunk, R., Flynn, M. J., Furneaux, K. L., Gallagher, M. W., Heard, D. E., Hollingsworth, A. M.,
5 Hornsby, K., Ingham, T., Jones, C. E., Jones, R. L., Kramer, L. J., Langridge, J. M., Leblanc, C.,
6 LeCrane, J. P., Lee, J. D., Leigh, R. J., Longley, I., Mahajan, A. S., Monks, P. S., Oetjen, H., Orr-
7 Ewing, A. J., Plane, J. M. C., Potin, P., Shillings, A. J. L., Thomas, F., von Glasow, R., Wada, R.,
8 Whalley, L. K., and Whitehead, J. D.: Iodine-mediated coastal particle formation: an overview of
9 the Reactive Halogens in the Marine Boundary Layer (RHAMBLE) Roscoff coastal study, *Atmos*
10 *Chem Phys*, 10, 2975-2999, 10.5194/acp-10-2975-2010, 2010.

11 Middlebrook, A. M., Murphy, D. M., and Thomson, D. S.: Observations of organic material in
12 individual marine particles at Cape Grim during the First Aerosol Characterization Experiment
13 (ACE 1), *J Geophys Res-Atmos*, 103, 16475-16483, Doi 10.1029/97jd03719, 1998.

14 Monks, P. S.: A review of the observations and origins of the spring ozone maximum, *Atmos*
15 *Environ*, 34, 3545-3561, Doi 10.1016/S1352-2310(00)00129-1, 2000.

16 Mäkelä, J. M., Maso, M. D., Pirjola, L., Keronen, P., Laakso, L., Kulmala, M., and Laaksonen, A.:
17 Characteristics of the atmospheric particle formation events observed at a boreal forest site in
18 Southern Finland, *Boreal Environment Research*, 5, 299-313, 2000.

19 Nguyen, Q. T., Skov, H., Sørensen, L. L., Jensen, B. J., Grube, A. G., Massling, A., Glasius, M.,
20 and Nøjgaard, J. K.: Source apportionment of particles at Station Nord, North East Greenland
21 during 2008–2010 using COPREM and PMF analysis, *Atmos Chem Phys*, 13, 35-49, 10.5194/acp-
22 13-35-2013, 2013.

23 Nguyen, Q. T., Kristensen, T. B., Hansen, A. M. K., Skov, H., Bossi, R., Massling, A., Sorensen, L.
24 L., Bilde, M., Glasius, M., and Nøjgaard, J. K.: Characterization of humic-like substances in Arctic
25 aerosols, *J Geophys Res-Atmos*, 119, 5011-5027, Doi 10.1002/2013jd020144, 2014.

26 O'Dowd, C. D., Hameri, K., Makela, J. M., Pirjola, L., Kulmala, M., Jennings, S. G., Berresheim,
27 H., Hansson, H. C., de Leeuw, G., Kunz, G. J., Allen, A. G., Hewitt, C. N., Jackson, A., Viisanen,
28 Y., and Hoffmann, T.: A dedicated study of New Particle Formation and Fate in the Coastal
29 Environment (PARFORCE): Overview of objectives and achievements, *J Geophys Res-Atmos*,
30 107, 10.1029/2001jd000555, 2002.

31 Odowd, C. D., and Smith, M. H.: Physicochemical Properties of Aerosols over the Northeast
32 Atlantic - Evidence for Wind-Speed-Related Submicron Sea-Salt Aerosol Production, *J Geophys*
33 *Res-Atmos*, 98, 1137-1149, Doi 10.1029/92jd02302, 1993.

34 Pfeifer, S., Birmili, W., Schladitz, A., Muller, T., Nowak, A., and Wiedensohler, A.: A fast and
35 easy-to-implement inversion algorithm for mobility particle size spectrometers considering particle
36 number size distribution information outside of the detection range, *Atmos Meas Tech*, 7, 95-105,
37 10.5194/amt-7-95-2014, 2014.

1 Pirjola, L., O'Dowd, C. D., Brooks, I. M., and Kulmala, M.: Can new particle formation occur in the
2 clean marine boundary layer?, *J Geophys Res-Atmos*, 105, 26531-26546, Doi
3 10.1029/2000jd900310, 2000.

4 Pnyushkov, A. V., Polyakov, I. V., Ivanov, V. V., and Kikuchi, T.: Structure of the Fram Strait
5 branch of the boundary current in the Eurasian Basin of the Arctic Ocean, *Polar Sci*, 7, 53-71,
6 10.1016/j.polar.2013.02.001, 2013.

7 Pratt, K. A., Custard, K. D., Shepson, P. B., Douglas, T. A., Pohler, D., General, S., Zielcke, J.,
8 Simpson, W. R., Platt, U., Tanner, D. J., Gregory Huey, L., Carlsen, M., and Stirm, B. H.:
9 Photochemical production of molecular bromine in Arctic surface snowpacks, *Nature Geosci*, 6,
10 351-356, 10.1038/ngeo1779 2013.

11 Pryor, S. C., Spaulding, A. M., and Barthelmie, R. J.: New particle formation in the Midwestern
12 USA: Event characteristics, meteorological context and vertical profiles, *Atmos Environ*, 44, 4413-
13 4425, DOI 10.1016/j.atmosenv.2010.07.045, 2010.

14 Quinn, P. K., Miller, T. L., Bates, T. S., Ogren, J. A., Andrews, E., and Shaw, G. E.: A 3-year
15 record of simultaneously measured aerosol chemical and optical properties at Barrow, Alaska, *J*
16 *Geophys Res-Atmos*, 107, Doi 10.1029/2001jd001248, 2002.

17 Quinn, P. K., Bates, T. S., Baum, E., Doubleday, N., Fiore, A. M., Flanner, M., Fridlind, A.,
18 Garrett, T. J., Koch, D., Menon, S., Shindell, D., Stohl, A., and Warren, S. G.: Short-lived
19 pollutants in the Arctic: their climate impact and possible mitigation strategies, *Atmos Chem Phys*,
20 8, 1723-1735, DOI 10.5194/acp-8-1723-2008, 2008.

21 Riipinen, I., Pierce, J. R., Yli-Juuti, T., Nieminen, T., Hakkinen, S., Ehn, M., Junninen, H.,
22 Lehtipalo, K., Petaja, T., Slowik, J., Chang, R., Shantz, N. C., Abbatt, J., Leaitch, W. R., Kerminen,
23 V. M., Worsnop, D. R., Pandis, S. N., Donahue, N. M., and Kulmala, M.: Organic condensation: a
24 vital link connecting aerosol formation to cloud condensation nuclei (CCN) concentrations, *Atmos*
25 *Chem Phys*, 11, 3865-3878, DOI 10.5194/acp-11-3865-2011, 2011.

26 Riipinen, I., Yli-Juuti, T., Pierce, J. R., Petaja, T., Worsnop, D. R., Kulmala, M., and Donahue, N.
27 M.: The contribution of organics to atmospheric nanoparticle growth, *Nat Geosci*, 5, 453-458, Doi
28 10.1038/Ngeo1499, 2012.

29 Saiz-Lopez, A., and von Glasow, R.: Reactive halogen chemistry in the troposphere, *Chem Soc*
30 *Rev*, 41, 6448-6472, 10.1039/c2cs35208g, 2012.

31 Sellegri, K., O'Dowd, C. D., Yoon, Y. J., Jennings, S. G., and de Leeuw, G.: Surfactants and
32 submicron sea spray generation, *J Geophys Res-Atmos*, 111, Artn D22215 Doi
33 10.1029/2005jd006658, 2006.

34 Shupe, M. D., and Intrieri, J. M.: Cloud radiative forcing of the Arctic surface: The influence of
35 cloud properties, surface albedo, and solar zenith angle, *J Climate*, 17, 616-628, Doi 10.1175/1520-
36 0442(2004)017<0616:Crfota>2.0.Co;2, 2004.

37 Simpson, W. R., von Glasow, R., Riedel, K., Anderson, P., Ariya, P., Bottenheim, J., Burrows, J.,
38 Carpenter, L. J., Friess, U., Goodsite, M. E., Heard, D., Hutterli, M., Jacobi, H. W., Kaleschke, L.,
39 Neff, B., Plane, J., Platt, U., Richter, A., Roscoe, H., Sander, R., Shepson, P., Sodeau, J., Steffen,

- 1 A., Wagner, T., and Wolff, E.: Halogens and their role in polar boundary-layer ozone depletion,
2 *Atmos Chem Phys*, 7, 4375-4418, 2007.
- 3 Singh, H. B., Kanakidou, M., Crutzen, P. J., and Jacob, D. J.: High-Concentrations and
4 Photochemical Fate of Oxygenated Hydrocarbons in the Global Troposphere, *Nature*, 378, 50-54,
5 Doi 10.1038/378050a0, 1995.
- 6 Skov, H., Christensen, J. H., Goodsite, M. E., Heidam, N. Z., Jensen, B., Wahlin, P., and Geernaert,
7 G.: Fate of elemental mercury in the arctic during atmospheric mercury depletion episodes and the
8 load of atmospheric mercury to the arctic, *Environ Sci Technol*, 38, 2373-2382,
9 10.1021/es030080h, 2004.
- 10 Stendel, M., Christensen, J. H., and Petersen, D.: Arctic climate and climate change with a focus on
11 Greenland, *Adv Ecol Res*, 40, 13-43, 10.1016/S0065-2504(07)00002-5, 2008.
- 12 Stroeve, J., Serreze, M., Holland, M., Kay, J., Malanik, J., and Barrett, A.: The Arctic's rapidly
13 shrinking sea ice cover: a research synthesis, *Climatic Change*, 110, 1005-1027, 10.1007/s10584-
14 011-0101-1, 2012.
- 15 Ström, J., Umegard, J., Torseth, K., Tunved, P., Hansson, H. C., Holmen, K., Wismann, V., Herber,
16 A., and König-Langlo, G.: One year of particle size distribution and aerosol chemical composition
17 measurements at the Zeppelin Station, Svalbard, March 2000-March 2001, *Physics and Chemistry
18 of the Earth*, 28, 1181-1190, DOI 10.1016/j.pce.2003.08.058, 2003.
- 19 Tervahattu, H., Juhanaja, J., and Kupiainen, K.: Identification of an organic coating on marine
20 aerosol particles by TOF-SIMS, *J Geophys Res-Atmos*, 107, Artn 4319 Doi
21 10.1029/2001jd001403, 2002.
- 22 Tunved, P., Ström, J., and Krejci, R.: Arctic aerosol life cycle: linking aerosol size distributions
23 observed between 2000 and 2010 with air mass transport and precipitation at Zeppelin station, Ny-
24 Ålesund, Svalbard, *Atmos. Chem. Phys.*, 13, 3643-3660, 10.5194/acp-13-3643-2013, 2013.
- 25 Vehkamäki, H., Dal Maso, M., Hussein, T., Flanagan, R., Hyvärinen, A., Lauros, J., Merikanto, J.,
26 Monkkonen, P., Pihlatie, M., Salminen, K., Sogacheva, L., Thum, T., Ruuskanen, T. M., Keronen,
27 P., Aalto, P. P., Hari, P., Lehtinen, K. E. J., Rannik, U., and Kulmala, M.: Atmospheric particle
28 formation events at Varri measurement station in Finnish Lapland 1998-2002, *Atmos Chem Phys*,
29 4, 2015-2023, 2004.
- 30 Vaananen, R., Kyro, E. M., Nieminen, T., Kivekas, N., Junninen, H., Virlikula, A., Dal Maso, M.,
31 Lihavainen, H., Viisanen, Y., Svenningsson, B., Holst, T., Arneth, A., Aalto, P. P., Kulmala, M.,
32 and Kerminen, V. M.: Analysis of particle size distribution changes between three measurement
33 sites in northern Scandinavia, *Atmos Chem Phys*, 13, 11887-11903, DOI 10.5194/acp-13-11887-
34 2013, 2013.
- 35 Walker, T. W., Jones, D. B. A., Parrington, M., Henze, D. K., Murray, L. T., Bottenheim, J. W.,
36 Anlauf, K., Worden, J. R., Bowman, K. W., Shim, C., Singh, K., Kopacz, M., Tarasick, D. W.,
37 Davies, J., von der Gathen, P., Thompson, A. M., and Carouge, C. C.: Impacts of midlatitude
38 precursor emissions and local photochemistry on ozone abundances in the Arctic, *J Geophys Res-
39 Atmos*, 117, Artn D01305 Doi 10.1029/2011jd016370, 2012.

1 Wiedensohler, A., Covert, D. S., Swietlicki, E., Aalto, P., Heintzenberg, J., and Leck, C.:
2 Occurrence of an ultrafine particle mode less than 20 nm in diameter in the marine boundary layer
3 during Arctic summer and autumn, *Tellus B*, 48, 213-222, DOI 10.1034/j.1600-0889.1996.t01-1-
4 00006.x, 1996.

5 Wiedensohler, A., Birmili, W., Nowak, A., Sonntag, A., Weinhold, K., Merkel, M., Wehner, B.,
6 Tuch, T., Pfeifer, S., Fiebig, M., Fjaraa, A. M., Asmi, E., Sellegri, K., Depuy, R., Venzac, H.,
7 Villani, P., Laj, P., Aalto, P., Ogren, J. A., Swietlicki, E., Williams, P., Roldin, P., Quincey, P.,
8 Huglin, C., Fierz-Schmidhauser, R., Gysel, M., Weingartner, E., Riccobono, F., Santos, S.,
9 Gruning, C., Faloon, K., Beddows, D., Harrison, R. M., Monahan, C., Jennings, S. G., O'Dowd, C.
10 D., Marinoni, A., Horn, H. G., Keck, L., Jiang, J., Scheckman, J., McMurry, P. H., Deng, Z., Zhao,
11 C. S., Moerman, M., Henzing, B., de Leeuw, G., Loschau, G., and Bastian, S.: Mobility particle size
12 spectrometers: harmonization of technical standards and data structure to facilitate high quality
13 long-term observations of atmospheric particle number size distributions, *Atmos Meas Tech*, 5,
14 657-685, DOI 10.5194/amt-5-657-2012, 2012.

15 Winklmayr, W., Reischl, G. P., Lindner, A. O., and Berner, A.: A New Electromobility
16 Spectrometer for the Measurement of Aerosol Size Distributions in the Size Range from 1 to 1000
17 Nm, *J Aerosol Sci*, 22, 289-296, 1991.

18 Ziemba, L. D., Dibb, J. E., Griffin, R. J., Huey, L. G., and Beckman, P.: Observations of particle
19 growth at a remote, Arctic site, *Atmos Environ*, 44, 1649-1657, DOI
20 10.1016/j.atmosenv.2010.01.032, 2010.

21 Zwally, H. J., Abdalati, W., Herring, T., Larson, K., Saba, J., and Steffen, K.: Surface melt-induced
22 acceleration of Greenland ice-sheet flow, *Science*, 297, 218-222, DOI 10.1126/science.1072708,
23 2002.

24

1 **List of Figures**

2 **Fig. 1.** The high Arctic site Villum Research Station, Station Nord (81°36' N, 16°40'W, 30 m a.s.l.)
3 in northeast Greenland. The main measurement site is Flyger's hut, which is located about 2.5 km
4 southeast of the Danish military base.

5 **Fig. 2.** SMPS, O₃ and NO_x data coverage at Station Nord from July 2010 - February 2013.

6 **Fig. 3.** Time series of particle number size distributions as dN/dlogDp (cm⁻³) during 2012. The
7 original 5 min time resolution was used in the plots.

8 **Fig. 4.** Monthly median particle number size distribution at Station Nord during 2012. The
9 corresponding lognormal-fitting parameters are shown in **Table 21**. The shade area shows the 75th
10 (upper) and 25th (lower) percentile of the actual data.
11

12 **Fig. 5.** Windroses showing monthly wind direction and wind speed at Station Nord during 2012.
13 The concentric rings show the percentage of wind arriving from a particular direction.

14 **Fig. 6.** Demonstration of the impacts of O₃, NO and NO_x on the summer new particle formation
15 events occurring on June 15-20 (Event A), Aug 2 (Event B) and Aug 9-10 (Event C) in 2012.

16 **Fig. 7.** Demonstration of air mass back trajectories calculated hourly using HYSPLIT for arrival at
17 50 m and 500 m at the station for the case study events.

18 ~~Demonstration of air mass back trajectories calculated using HYSPLIT for arrival at 50 m and 500~~
19 ~~m at the station on selected days with new particle formation events.~~

20 **Fig. 8.** The probability of observing an event at Station Nord (bottom tip of the black triangle) as a
21 function of air mass origin. This figure uses all available data (62 events) from the study period July
22 2010 – February 2013.

23 **Fig. 9.** Monthly variation of total number of days with good data (left vertical axis) and frequency
24 percentages (%) of event days, non-event days and undefined days (right vertical axis) during the
25 study period (July 2010 - February 2013).

26

27

28

1 **List of Tables**

Formatted: Line spacing: 1.5 lines

2 **Table 1.** Three modes were fitted to the average monthly data of 2012 using lognormal fitting. The
3 parameters shown for each mode include the modal number concentration (N , cm^{-3}), the modal
4 geometrical mean diameter (D_g , nm) and the modal geometrical standard deviation (GSD). A fitted
5 sum of three lognormal distributions was calculated for the entire particle size range (averaged
6 monthly particle number size distributions) and the difference of the sum of the squares of each
7 number concentration at the specific sizes between the real and the fitted data was minimized using
8 the Excel solver add-in.

9 **Table 2.** Median and average particle number concentration (N), particle volume concentration (V)
10 and particle mass concentration (M) for the 12 months of 2012. M was calculated from V assuming
11 a density of 1.4 g cm^{-3} and particle sphericity.

12 **Table 3.** Percentage of total new particle formation events (marked in blue) versus non-events and
13 undefined days during the period July 2010 to February 2013. The total events were further divided
14 into Class I and Class II events. A column of total days (by month) over the studied years was also
15 provided.

16 **Supplementary Fig. 1.** Onset hour of NPF events based on 62 NPF events observed during the
17 period July 2010 – February 2013.

18 **Supplementary Fig. 2.** Arctic sea ice map on August 2, 2012. Source: Daily Arctic Sea Ice Maps.
19 URL: <http://arctic.atmos.uiuc.edu/cryosphere/>, Access date: June 15, 2016.

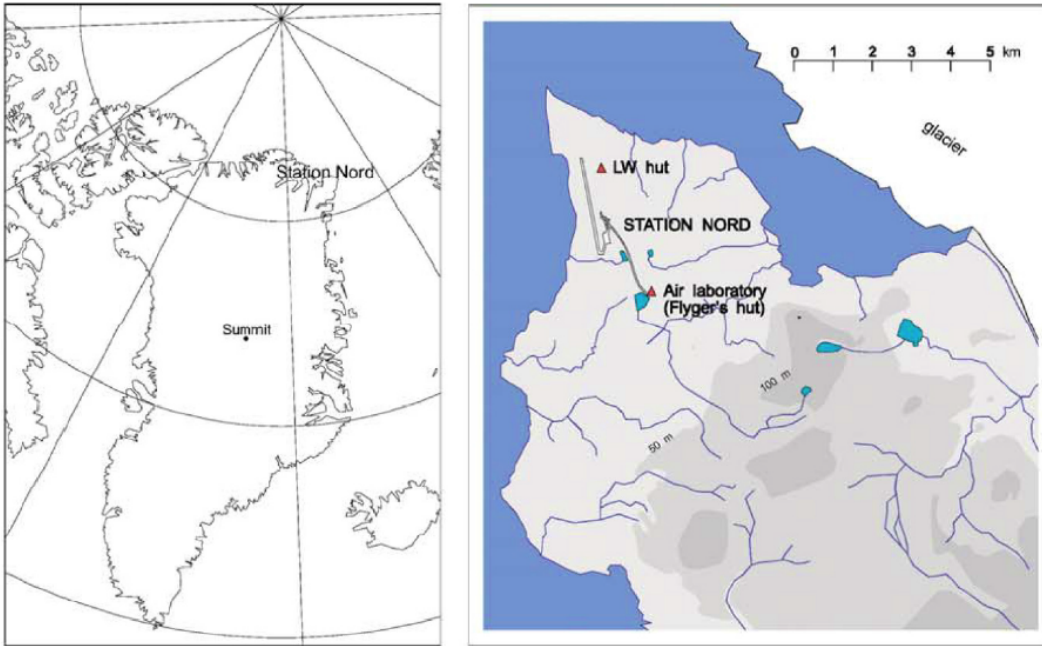
20

21

22

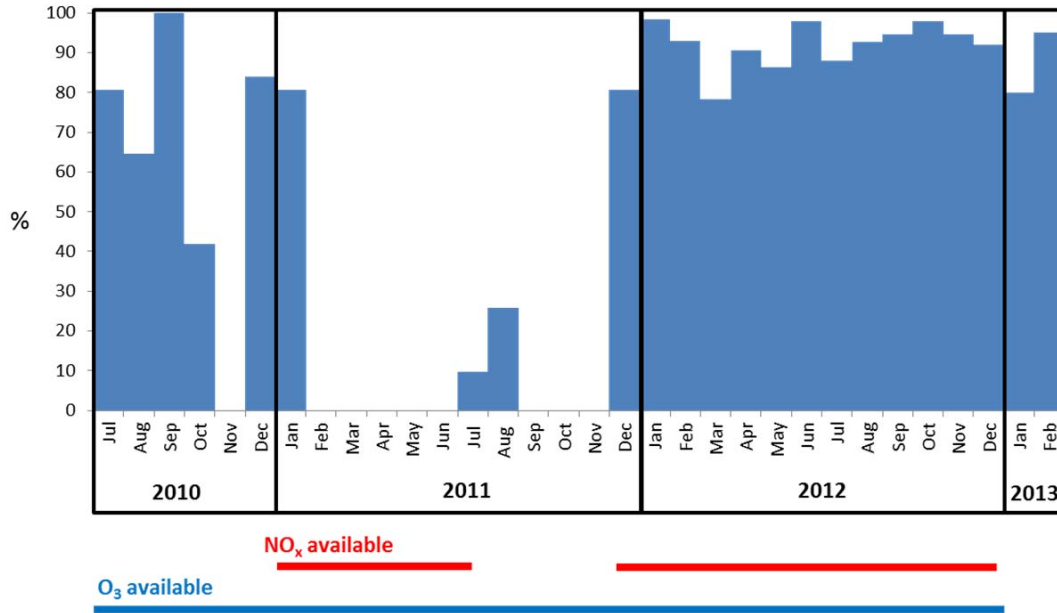
1 **Figures**

2 **Fig. 1.** The high Arctic site Villum Research Station, Station Nord (81°36' N, 16°40'W, 30 m a.s.l.)
3 in northeast Greenland. The main measurement site is Flyger's hut, which is located about 2.5 km
4 southeast of the Danish military base.



5
6

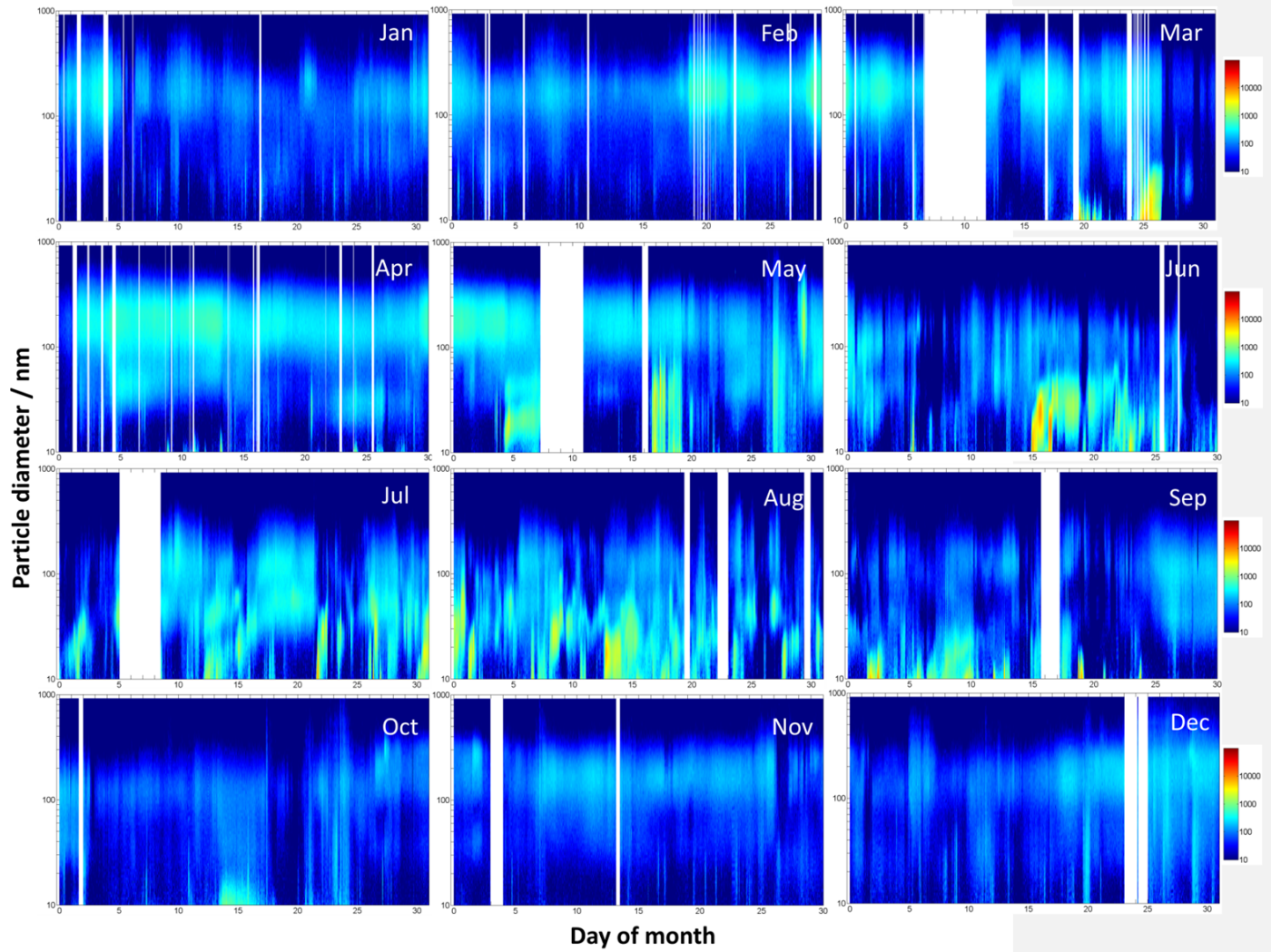
1 **Fig. 2.** SMPS, O₃ and NO_x data coverage at Station Nord from July 2010 - February 2013.



2

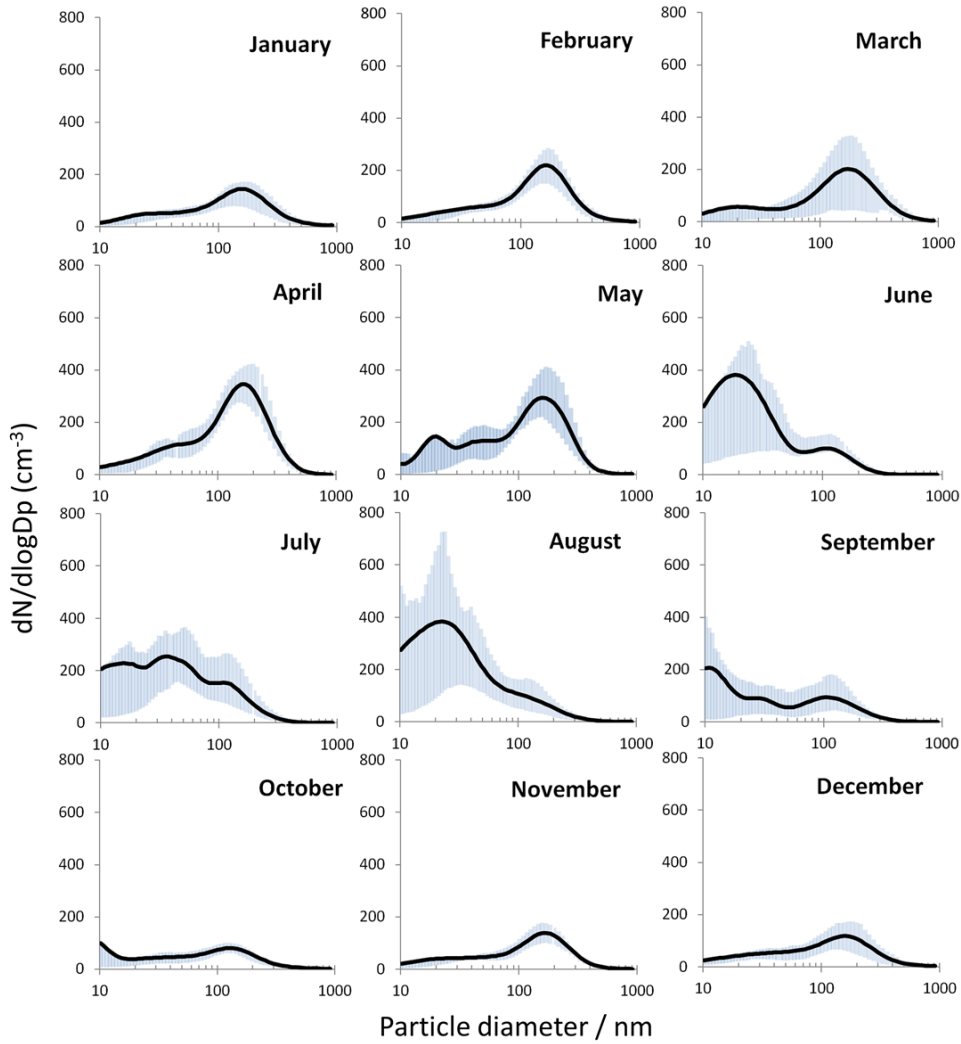
3

1 **Fig. 3.** Time series of particle number size distributions as $dN/d\log D_p$ (cm^{-3}) during 2012. The
2 original 5 min time resolution was used in the plots.
3



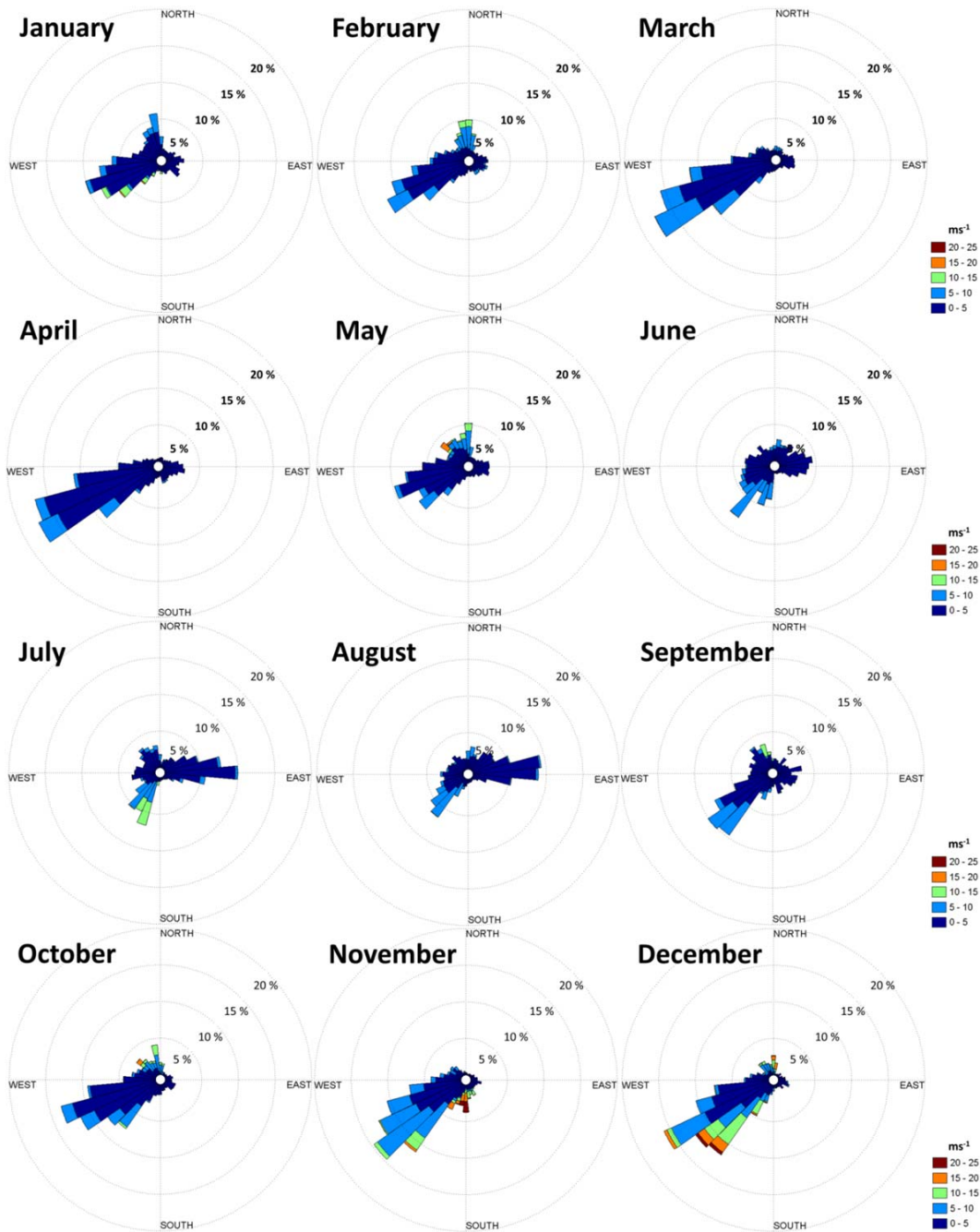
4
5

1 **Fig. 4.** Monthly median particle number size distribution at Station Nord during 2012. The
2 corresponding lognormal-fitting parameters are shown in **Table 12**. The shade area shows the 75th
3 (upper) and 25th (lower) percentile of the actual data.
4



5
6

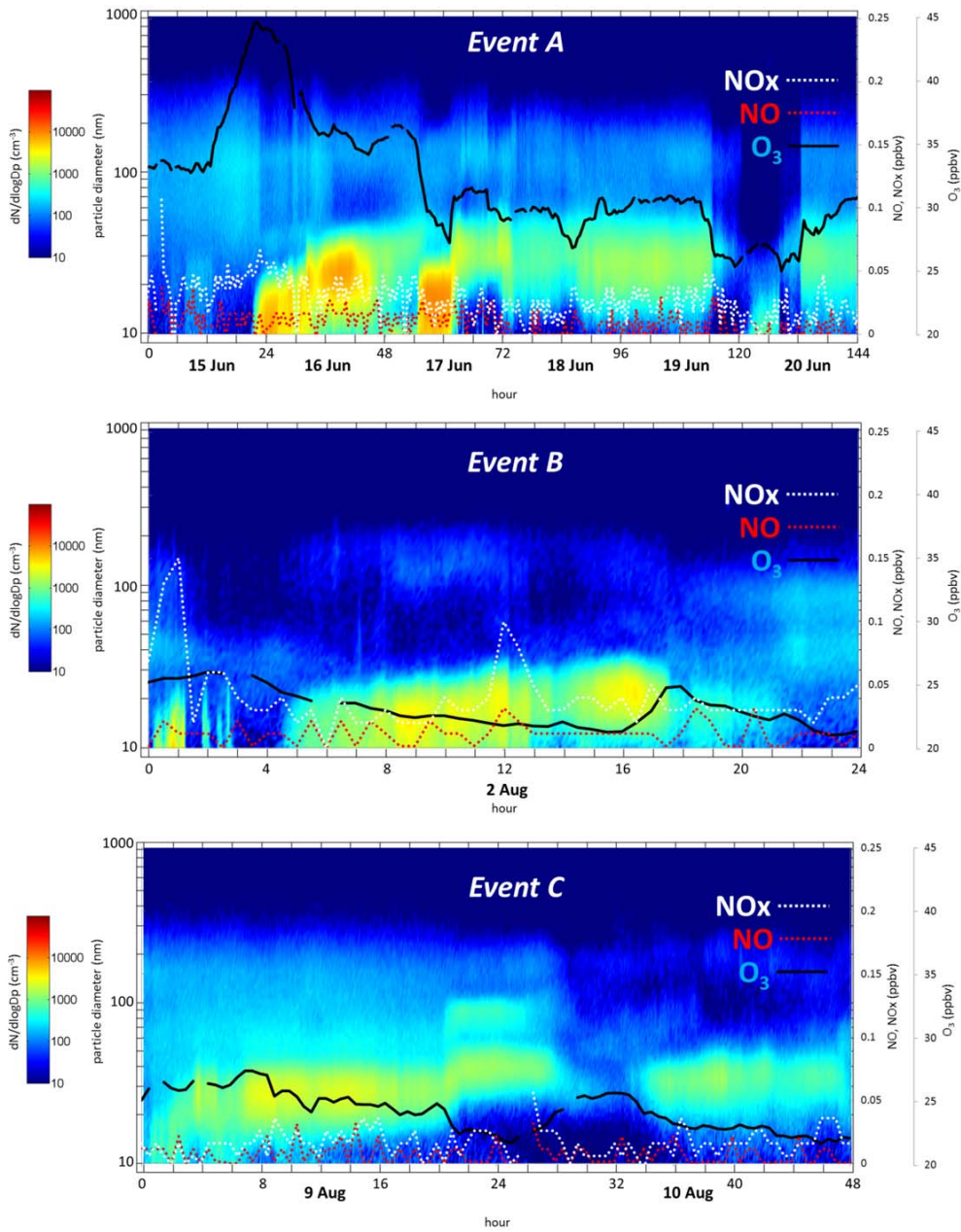
- 1 **Fig. 5.** Windroses showing monthly wind direction and wind speed at Station Nord during 2012.
- 2 The concentric rings show the percentage of wind arriving from a particular direction.



3

1 **Fig. 6.** Demonstration of the connection between O₃, NO and NO_x and summertime new particle
2 formation events occurring on June 15-20 (Event A), Aug 2 (Event B) and Aug 9-10 (Event C) in
3 2012.

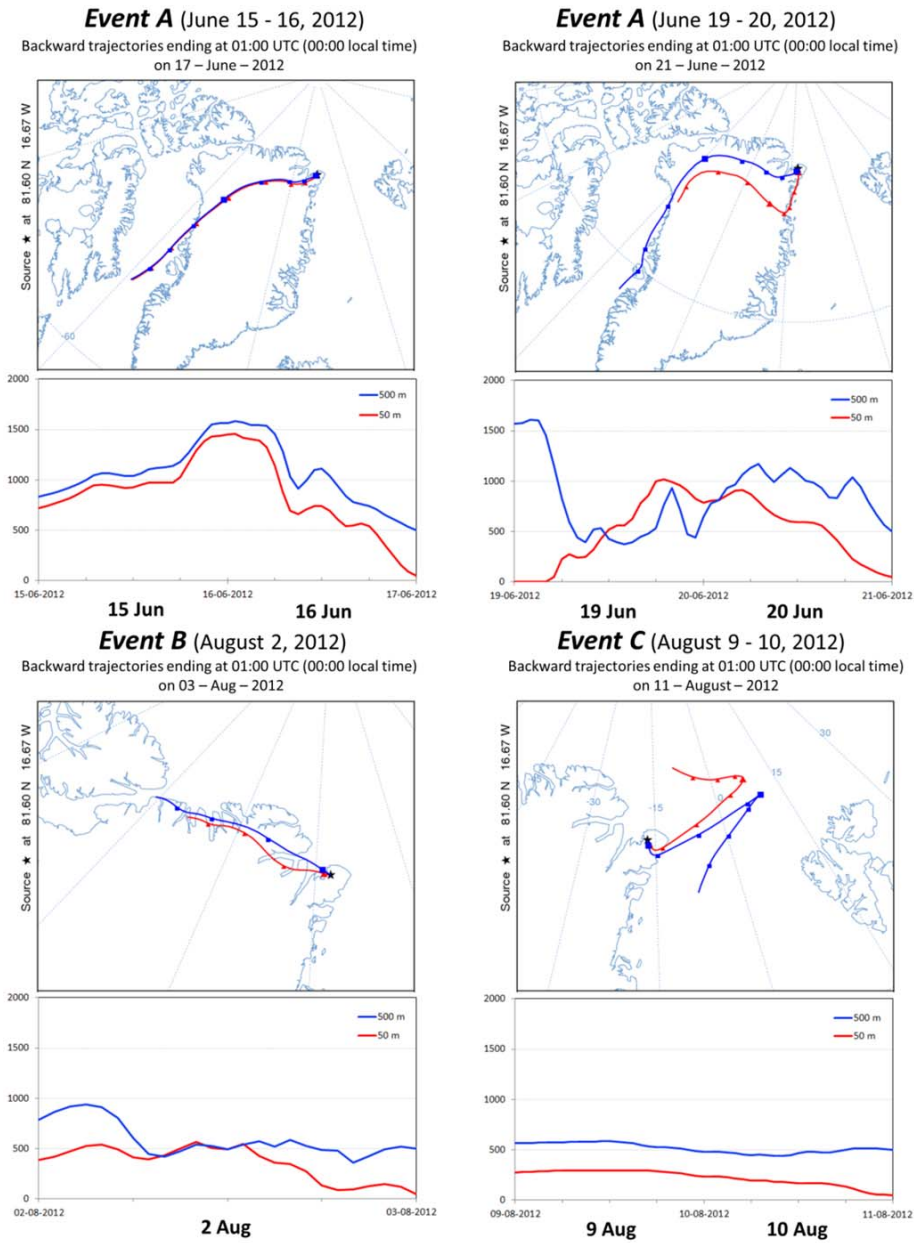
4



5

1
2

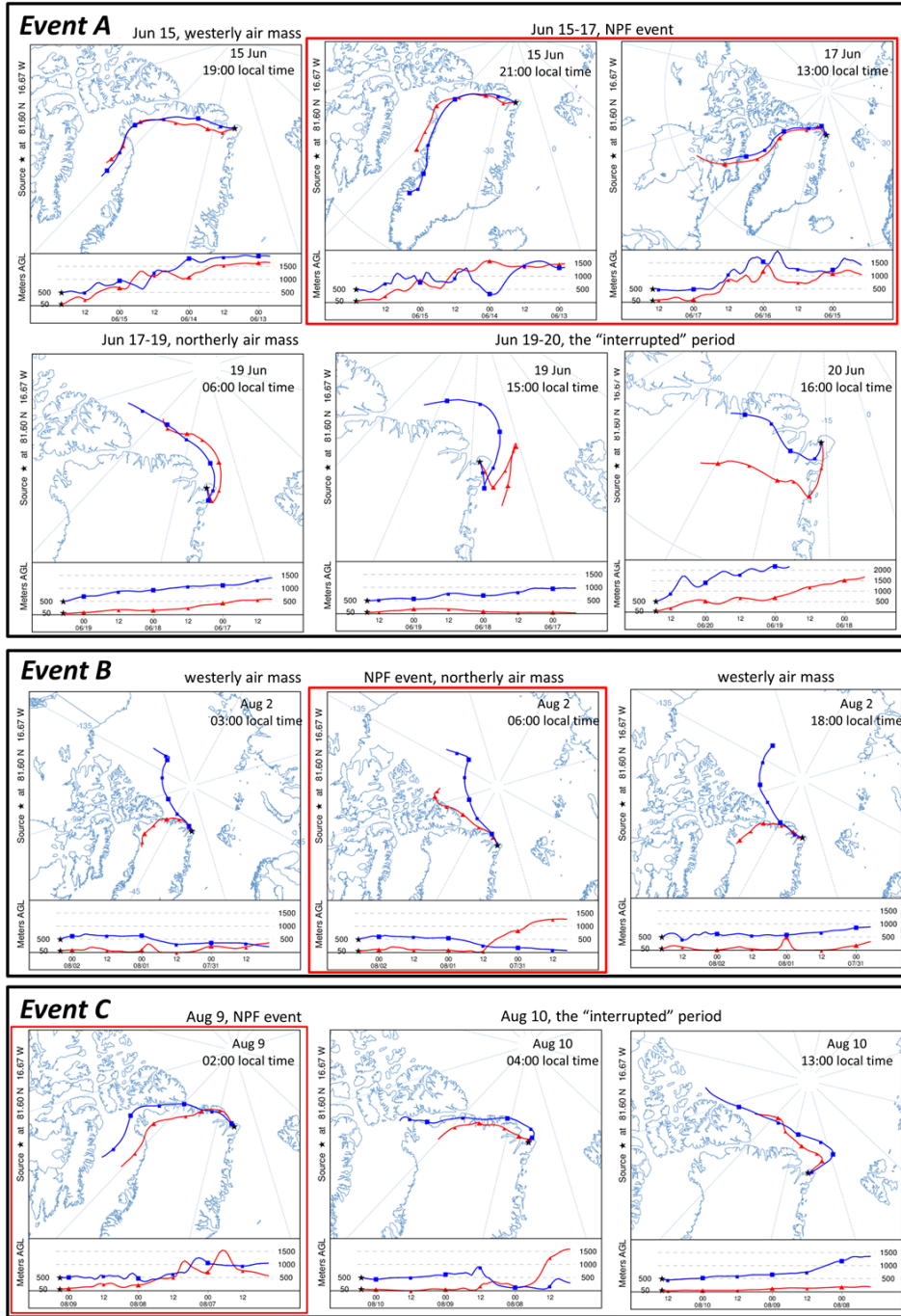
Fig. 7. Demonstration of air mass back trajectories calculated using HYSPLIT for arrival at 50 m and 500 m at the station on selected days with new particle formation events.



3
4
5
6

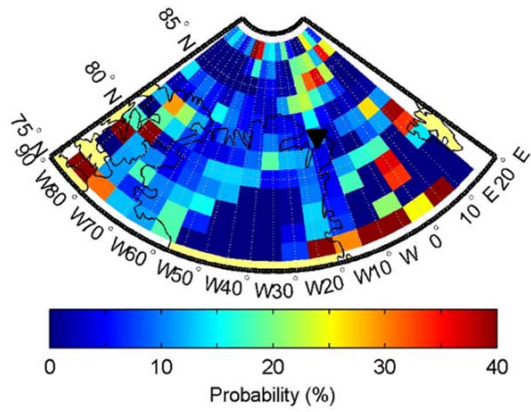
1
2

Fig. 7. Demonstration of air mass back trajectories calculated hourly using HYSPLIT for arrival at 50 m and 500 m at the station for the case study events.



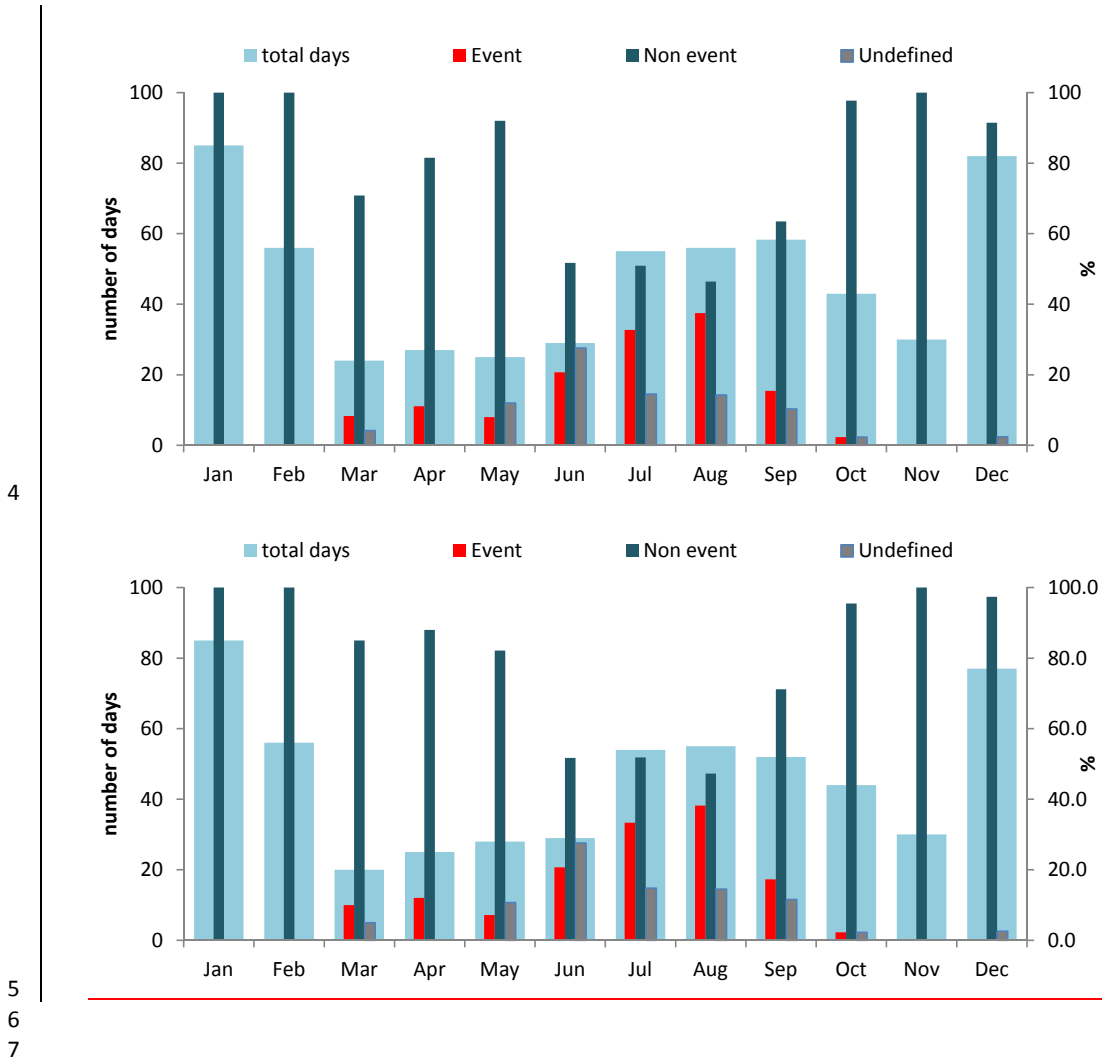
3
4

1 **Fig. 8.** The probability of observing an event at Station Nord (bottom tip of the black triangle) as a
2 function of air mass origin. [This figure uses all available data \(62 events\) from the study period July](#)
3 [2010 – February 2013.](#)
4



5
6

1 **Fig. 9.** Monthly variation of total number of days with good data (left vertical axis) and frequency
 2 percentages (%) of event days, non-event days and undefined days (right vertical axis) during the
 3 study period (July 2010 - February 2013).



1 **Table**

2 **Table 1.** Three modes were fitted to the average monthly data of 2012 using lognormal fitting. The
3 parameters shown for each mode include the modal number concentration (N , cm^{-3}), the modal
4 geometrical mean diameter (D_g , nm) and the modal geometrical standard deviation (GSD). A fitted
5 sum of three lognormal distributions was calculated for the entire particle size range (averaged
6 monthly particle number size distributions) and the difference of the sum of the squares of each
7 number concentration at the specific sizes between the real and the fitted data was minimized using
8 the Excel solver add-in.

	N_1 (cm^{-3})	$D_{g,1}$ (nm)	GSD ₁	N_2 (cm^{-3})	$D_{g,2}$ (nm)	GSD ₂	N_3 (cm^{-3})	$D_{g,3}$ (nm)	GSD ₃
January	5	22	1.4	72	68	3.3	50	167	1.6
February	22	27	2.2	58	97	2.7	75	169	1.5
March	24	17	1.7	49	84	2.8	93	179	1.7
April	45	24	2.4	38	48	1.6	172	167	1.6
May	17	18	1.2	134	43	2.5	125	173	1.5
June	252	17	1.9	22	31	1.4	45	113	1.5
July	196	21	2.6	24	45	1.3	50	119	1.6
August	287	16	2.3	51	30	1.5	49	114	1.8
September	90	11	1.5	25	29	1.4	57	107	1.8
October	25	9	1.3	60	41	3.3	24	139	1.5
November	12	16	1.7	45	62	2.6	51	173	1.5
December	31	22	2.4	48	100	2.5	35	170	1.5

9

10

1 **Table 2.** Median and average particle number concentration (N), particle volume concentration (V)
 2 and particle mass concentration (M) for the 12 months of 2012. M was calculated from V assuming
 3 a density of 1.4 g cm^{-3} and particle sphericity.

	Median N (cm^{-3})	Average N (cm^{-3})	Median V ($\mu\text{m}^3 \text{ cm}^{-3}$)	Average V ($\mu\text{m}^3 \text{ cm}^{-3}$)	Median M ($\mu\text{g m}^{-3}$)	Average M ($\mu\text{g m}^{-3}$)
January	104	121	0.44	0.69	0.61	0.96
February	123	149	0.69	0.82	0.97	1.15
March	170	174	1.10	1.13	1.54	1.58
April	231	253	0.88	0.93	1.24	1.30
May	221	268	0.78	0.78	1.09	1.09
June	137	277	0.14	0.15	0.20	0.21
July	229	237	0.17	0.20	0.23	0.29
August	227	313	0.19	0.21	0.27	0.29
September	124	137	0.18	0.18	0.25	0.25
October	71	87	0.17	0.25	0.24	0.35
November	96	100	0.40	0.42	0.55	0.59
December	85	107	0.30	0.57	0.42	0.80

4
 5
 6
 7

1 **Table 3.** Percentage of total new particle formation events (marked in blue) versus non-events and
 2 undefined days during the period July 2010 to February 2013. The total events were further divided
 3 into Class I and Class II events. A column of total days (by month) over the studied years was also
 4 provided.

	Total days	Class I (%)	Class II (%)	Total events (%)	Non-events (%)	Undefined (%)
January	85	0	0	0	100.0	0
February	56	0	0	0	100.0	0
March	204	0	8 10.0	8 10.0	71 85.0	45.0
April	257	0	4 12.0	4 12.0	8 88.0	0
May	285	0	8 7.1	8 7.1	92 82.1	12 10.7
June	29	7 6.9	4 13.8	2 120.7	5 251.7	2 827.6
July	545	9 3	24 1	33 3	51 9	45 14.8
August	556	9 1	29 1	38 2	46 47.3	14 5
September	528	5 8	40 11.5	45 17.3	63 71.2	40 11.5
October	443	0	2 3	2 3	98 95.5	2 3
November	30	0	0	0	100.0	0
December	7782	0	0	0	91 97.4	2 6
Total	570	32 6	9 2	11 7	79 80.8	7 4

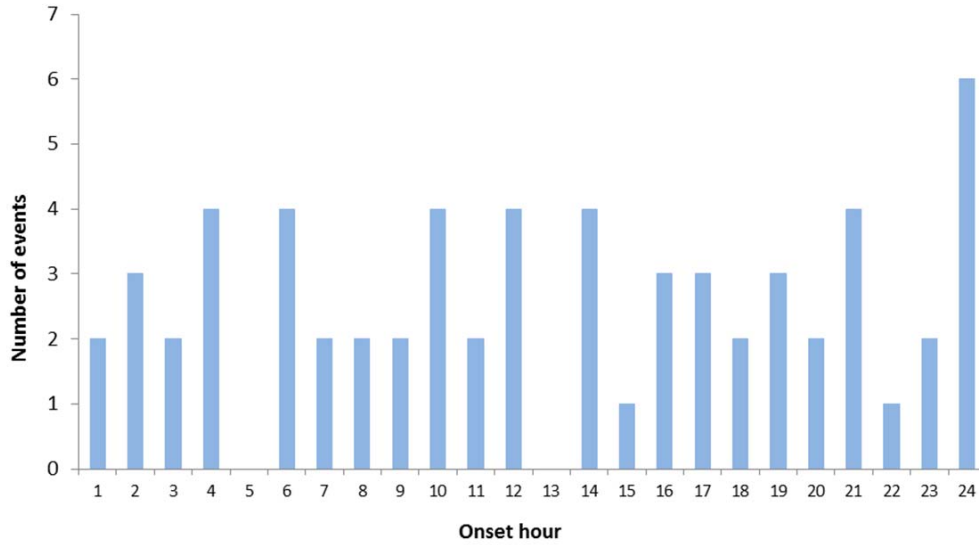
5

6

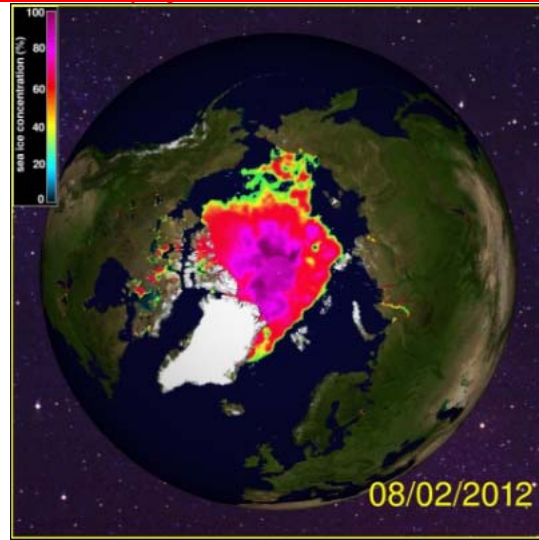
7

8

1 **Supplementary Fig. 1.** Onset hour of NPF events based on 62 NPF events observed during the
2 period July 2010 – February 2013.



3 **Supplementary Fig. 2.** Arctic sea ice map on August 2, 2012. Source: Daily Arctic Sea Ice Maps,
4 URL: <http://arctic.atmos.uiuc.edu/cryosphere/>, Access date: June 15, 2016.



6